frontiers | Frontiers in Plant Science

TYPE Original Research
PUBLISHED 07 February 2023
DOI 10.3389/fpls.2023.1103241

OPEN ACCESS

EDITED BY
Awadhesh Kumar,
National Rice Research Institute (ICAR), India

REVIEWED BY
Soumya Kumar Sahoo,
Siksha O Anusandhan University, India
Goutam Kumar Dash,
Centurion University of Technology and Management, India

*CORRESPONDENCE
Yueming Yan
yanym@cnu.edu.cn

†These authors have contributed equally to this work

SPECIALTY SECTION
This article was submitted to Plant Abiotic Stress, a section of the journal Frontiers in Plant Science

RECEIVED 20 November 2022
ACCEPTED 20 January 2023
PUBLISHED 07 February 2023

CITATION
Luo F, Zhu D, Sun H, Zou R, Duan W, Liu J and Yan Y (2023) Wheat Selenium-binding protein TaSBP-A enhances cadmium tolerance by decreasing free Cd^{2+} and alleviating the oxidative damage and photosynthesis impairment.
Front. Plant Sci. 14:1103241.
doi: 10.3389/fpls.2023.1103241

Wheat Selenium-binding protein TaSBP-A enhances cadmium tolerance by decreasing free Cd^{2+} and alleviating the oxidative damage and photosynthesis impairment

Fei Luo†, Dong Zhu†, Haocheng Sun†, Rong Zou, Wenjing Duan, Junxian Liu and Yueming Yan*

Beijing Key Laboratory of Plant Gene Resources and Biotechnology for Carbon Reduction and Environmental Improvement, College of Life Science, Capital Normal University, Beijing, China

Cadmium, one of the toxic heavy metals, robustly impact crop growth and development and food safety. In this study, the mechanisms of wheat (*Triticum aestivum* L.) selenium-binding protein-A (TaSBP-A) involved in response to Cd stress was fully investigated by overexpression in Arabidopsis and wheat. As a cytoplasm protein, TaSBP-A showed a high expression in plant roots and its expression levels were highly induced by Cd treatment. The overexpression of *TaSBP-A* enhanced Cd-toleration in yeast, Arabidopsis and wheat. Meanwhile, transgenic Arabidopsis under Cd stress showed a lower H_2O_2 and malondialdehyde content and a higher photochemical efficiency in the leaf and a reduction of free Cd^{2+} in the root. Transgenic wheat seedlings of TaSBP exhibited an increment of Cd content in the root, and a reduction Cd content in the leaf under Cd^{2+} stress. Cd^{2+} binding assay combined with a thermodynamics survey and secondary structure analysis indicated that the unique CXXC motif in TaSBP was a major Cd-binding site participating in the Cd detoxification. These results suggested that TaSBP-A can enhance the sequestration of free Cd^{2+} in root and inhibit the Cd transfer from root to leaf, ultimately conferring plant Cd-tolerance *via* alleviating the oxidative stress and photosynthesis impairment triggered by Cd stress.

KEYWORDS

wheat, Selenium-binding protein, Cd tolerance, oxidative stress, photosynthesis impairment, CXXC motif

Introduction

As an allohexaploid species, wheat (*Triticum aestivum* L., 2n=6x=42, AABBDD) has a wide adaptability and provides a stable source of carbohydrates and proteins duo to its uncommon genetic potential that synchronizes its flowering time with diverse environmental conditions (Kamran et al., 2014). Wheat consumption is globally estimated to rise 70% in the next few decades (2020–2050) as the human population increases (Vitale et al., 2020).

However, many anthropogenic industrial activities including electroplating, mining, battery production and iron and steel plants as well as widely used pesticides and phosphate fertilizers in modern agriculture are some of major sources of heavy metal such as cadmium (Cd), chromium (Cr), mercury (Hg), lead (Pb), copper (Cu), zinc (Zn) and nickel (Ni) to soils (Choppala et al., 2013; Haider et al., 2021; Qin et al., 2021). Those increasingly deteriorative contaminations in agricultural soils have become a serious threat to grain production worldwide (Rizwan et al., 2012; Caparrós et al, 2022). It is estimated that 12 million tons of grain are polluted each year by heavy metals in China (Qin et al., 2021). Among of those heavy metal, the accumulation of Cd was continuously increasing, while others was gradually decreasing during the period from 2005 to 2017 (Huang et al., 2019). Cd generally poses high toxicity to both plants that and humans, even at a very low concentration (López-Luna et al., 2015). The accumulation of Cd between 5–10 mg Cd kg^{-1} (dry matter) in plant tissue is toxic to most plants (Choppala et al., 2014). For human, the maximum dietary exposure of Cd is 25 μg kg^{-1} body weight per month according to FAO/WHO. Humans often contact with Cd-polluted foods *via* the food chain (Dai et al., 2012). When exposed to Cd contaminated environments, people would have a high risk of acquiring many diseases, including chronic kidney disease, osteoporosis, cardiovascular diseases, and cancer (Fatima et al., 2019). Therefore, it is significant to ensure food safety and human health to pay attention to heavy metal pollution, especially Cd- contaminations.

Cd stress has significant effects on plant growth and development at both morphological and physiological levels (Shanying et al., 2017). In morphological level, Cd toxicity was reported to cause a substantial decrease in total leaf area, root length and tips, and dry weight of plant leaves, stems and roots (Jinadasa et al., 2016; Rizwan et al., 2017). In physiological level, Cd stress causes damages in photosynthetic apparatus and Calvin cycle related enzymes, resulting in a decline of photosynthesis and carbon assimilation rate (Pietrini et al., 2010; Ying et al., 2010). Furthermore, Cd stress can induce water stress, leading to decreases in stomatal conductance, transpiration rate, and relative-water content of plant leaves (Arasimowicz-Jelonek et al., 2011; Najeeb et al., 2011). The signal transduction induced by Cd generally triggers reactive oxygen species (ROS) production, which damages cellular organelles and biomolecules (Ranieri et al., 2005; Gratão et al., 2015). In addition, Cd stress has negative effects on plant mineral content by interfering with the intake of mineral nutrients such as zinc (Zn), iron (Fe), calcium (Ca), manganese (Mn), magnesium (Mg), copper (Cu), silicon (Si), and potassium (K) (Khan et al., 2015a; Jinadasa et al., 2016). In summary, the physiological disorders caused by excessive intake of Cd^{2+} under Cd stress often produce a severe inhibition of morphology and grain yield loss in agriculture (Li et al., 2015).

Plants have evolved different mechanisms to resist Cd stress during the long evolutionary process, including restricting metal uptake and enhancing their detoxification abilities (Choppala et al., 2014; Wei et al., 2022). When plants subject to heavy metal stress in the soil solution, the cell walls serve as the first barrier against metal toxicity (Lang and Wernitznig, 2011). The cell wall of the stems, leaves and fruits was reported to involve in Cd immobilization in bush beans and pepper (Xin and Huang, 2014; Xin et al., 2014). Once Cd enters the cytosol, plants can form metal chelates/complexes to minimize the concentration of free Cd^{2+} in the cytosol (Sarwar et al., 2010; Saraswat and Rai, 2011). So far, two principal peptides have been found to participate in chelating to Cd: phytochelatins and metallothioneins (Ismael et al., 2019). The thiol moieties of phytochelatins and cysteine-rich small polypeptides can chelate metal ions, including Cd, Cu, Zn and Ag etc. (Cobbett and Goldsbrough, 2002; Uraguchi et al., 2017). Meanwhile, metallothioneins belonging to cysteine-rich proteins with a low molecular mass can resist to Cu and Cd stresses (Jianmin and Goldsbrough, 1994). Additionally, the vacuoles/plastid sequestration and metal efflux mechanism also significantly contributes to enhance plant detoxification abilities to Cd stress (Ogawa et al., 2009; Wang et al., 2015). It is known that some metal transporters can mediate these processes, such as CAX2/4 (Korenkov et al., 2007), HMA1/3 (Lei et al., 2020; Zhang et al., 2020), MRP3 (Verbruggen et al., 2009), ABCC3/9/13 (Bhati et al., 2016; Yang et al., 2021), and metal efflux transporters PCR1/2 (Lin et al., 2020), PDR8 (Kim et al., 2007), and MATE (Li et al., 2002; Wang et al., 2015).

The transcriptional regulation is an important strategy for plant heavy metal stress response. To date, many Cd-responsive transcription factors in plants have been identified and characterized, such as Hsfs (Shim et al., 2009; Chen et al., 2020), ERFs (Lin et al., 2017), ORG3 (Xu et al., 2017), WRKYs (Cai et al., 2020), MYBs (Agarwal et al., 2020), and bHLHs (Yao et al., 2018), etc. As the key downstream effectors of Cd stress transcriptional pathways, these Cd-responsive transcription factors can trigger the expression of Cd-detoxification genes and converge Cd stress signals (Chmielowska-Bąk et al., 2014). In addition, a lot of metallochaperones can traffic metal ions in cytosol. Saccharomyces cerevisiae metal homeostasis factor (ATX1) can bind a single Cu ion by two cysteines in the MXCXXC motif (here M, X and C represents methionine, any amino acid and cysteine, respectively) (Lin and Culotta, 1995; Rousselot-Pailley et al., 2006). This motif is also present in numerous metal binding proteins, such as the P-type copper transporter CCC2 (Yuan et al., 1995), bacterial carriers for mercury ions MerP (Powlowski and Sahlman, 1999), copper chaperones for SOD1 CCS (Culotta et al., 1997), and the cadmium binding protein Cd19 (Suzuki et al., 2002).

Wheat, compared to other cereals such as maize and rice, can accumulate more Cd mainly *via* the roots and then transfer it from roots to aerial parts, contributing to enrichments in the grain eventually (Greger and Löfstedt, 2004; Jafarnejadi et al., 2011). Therefore, it is significant to understand the mechanism of wheat response to Cd stress, which may be managed to alleviate Cd uptake or accumulation, promoting wheat growth and improving grain yield and quality. During the past decades, a number of strategies, such as the selection of low Cd-accumulating wheat cultivars (Liu et al., 2020), exogenous application of plant growth regulators (Agami and Mohamed, 2013; Wang et al., 2017b), the use of inorganic amendments (Khan et al., 2015b; Naeem et al., 2018; Cheng et al., 2021; Ma et al., 2022), organic amendments, nanoparticles (Grüter et al., 2019) have been applied for the alleviation of Cd toxicity in wheat (Zhou and Li, 2022). Low-Cd or high Cd-resistance wheat cultivars were increasingly fostered with molecular genetics and breeding approaches developed rapidly. (Zaid et al., 2018). Cd tolerance was enhanced in rice expressing *TaHsfA4a* by upregulating metallothionein gene expression (Shim et al., 2009).

The *OsHMA3* overexpression highly inhibited Cd accumulation in wheat grain by decreasing root-to-shoot Cd translocation nearly 10-fold (Zhang et al., 2020). The overexpression of durum wheat TdSHN1 conferred Cd resistance by promoting the activities of superoxide dismutase (SOD) and catalases (Djemal and Khoudi, 2022).

The candidate genes related to enhance crop tolerance to heavy metals are urgently needed to ensure food safety. The selenium-binding protein (SBP) is a typical SBP56 family member, which was identified in *A. thaliana* (Dutilleul et al., 2008; Hugouvieux et al., 2009; Schild et al., 2014). Early studies identified SBP as a cytosolic selenium binding protein, named as SBP56 in mouse liver, which was found to bind selenium (Bansal et al., 1989; Bansal et al., 1990). It is involved in intra-Golgi protein transport in Mammalia (Porat et al., 2000), and the decreased levels of SBP1 are associated with epithelial cancers and breast cancer (Yang and Diamond, 2013). Selenium-binding protein in plants, first found in *Lotus japonicas*, participated in nodule formation during the symbiosis of plants and rhizobia (Flemetakis et al., 2002). AtSBP1 has been reported that it can interact with glutaredoxins AtGRXS14 and AtGRXS16 that contain a PICOT domain and belong to part of the plant's response to oxidative stress (Valassakis et al., 2019). It also served as an interacting partner of DAD1-LIKE LIPASE 3 (DALL3) that participated in the network of genes regulated by cadmium (Dervisi et al., 2020). The overexpression of *SBP1* in rice could improve plant tolerance to different pathogens (Sawada et al., 2004). In particular, overexpressing *AtSBP1* in Arabidopsis enhanced tolerance to Cd stress in both suspension cells (Sarry et al., 2006) and entire plants (Dutilleul et al., 2008). Meanwhile, *AtSBP1* can also participate in Zn, Cu and H_2O_2 stress responses (Hugouvieux et al., 2009). The Se-binding site $Cys^{21}Cys^{22}$ in AtSBP1 was identified, which could form SeCys [R-S-Se(II)-S-R] and confirmed Se tolerance (Schild et al., 2014). The overexpression of *AtSBP1* could produce greater Cd accumulation in Arabidopsis (Dutilleul et al., 2008), indicating that AtSBP1 could enhance the Cd uptake. However, the state (free or complex) of the accumulated Cd in the overexpressed plants remains unclear; this is critical as it will allow researchers to further understand the mechanisms of SBP for Cd tolerance.

In the current study, a comprehensive investigation was performed to reveal the molecular mechanisms of wheat TaSBP-A enhancing Cd tolerance. We focused on dissecting the detoxification function of TaSBP-A *via* a specific Cd-binding motif. Our purpose is to provide new insights into the Cd-tolerant mechanisms of plants, which could be beneficial for improving the Cd tolerance as well as reducing grain Cd accumulation of crop cultivars.

Materials and methods

Wheat materials, seedling cultivation and Cd treatment

Common wheat variety Chinese Spring (CS) was used as material, and the mature seeds were cultivated based on the previous report (Zhang et al., 2014). In brief, the seedings were cultivated in Hoagland solution. The Cd stress treatment at three-leaf stage was conducted using 50 μM $CdCl_2$ in Hoagland solution. Three biological replicates were set in both treatment and control, and the samples of roots, stems (crown to ligule) and leaves were respectively collected from 24, 48, 72 h treatments and control, and then immediately immerged into liquid nitrogen prior to use.

RNA-seq and RT-qPCR

The expression profiling of *TaSBP* genes in different organs including roots, stem axis, leaves was detected using the RNA-seq database of wheat (http://www.wheat-expression.com/genes/heatmap?gene_set=RefSeq1.1&genes=TraesCS3A02G422100%2CTraesCS3D02G417500%2CTraesCS3B02G457600). Total RNA isolation, cDNA synthesis and real-time quantitative polymerase chain reaction (RT-qPCR) were based on the previous report (Yu et al., 2016). The specific primers were shown in Table S3. The expression levels of *TaSBP* were presented as values relative to the corresponding control samples at the indicated times and conditions after normalization to *Ubqutin* (UBI) transcript levels.

Subcellular localization

The *TaSBP-A* gene clone, vector (16318) construction and leaf protoplast transformation of Chinese Spring were based on previous report (Zou et al., 2020). The specific primers were shown in Table S3. Confocal laser scanning microscope (Leica TCS SP5, Germany) was used for monitoring the GFP signal and chlorophyll red auto-fluorescence.

Overexpression of TaSBP-A in *Saccharomyces cerevisiae*

Saccharomyces cerevisiae strain DEY1457 (*MATα can1 his3 leu2 trp1 ura3 ade6*), kindly provided by Prof. Liping Yin, Capital Normal University, was used for heterologous expression of TaSBP-A protein. The full gene CDS of TaSBP-A was cloned in the destination vector pYES2 (Invitrogen). The specific primers were shown in Table S3. The empty vectors (EV) and combined vectors were respectively transformed into yeast strains DEY1457 following standard procedure (Invitrogen). Single colonies cultured in the exponential phase (OD 2.0) were diluted to six stepped concentration (OD 2, 2 x 10^{-1}, 2 x 10^{-2}, 2 x 10^{-3}, 2 x 10^{-4}, 2 x 10^{-5}) and drop on the dextrose-Ura solid medium with/without 30 μM Cd^{2+}. Three independent clones were used for the experiments.

Overexpression of TaSBP-A in Arabidopsis and wheat and Cd stress treatment

Arabidopsis genetic transformation was based on previous report (Li et al., 2017). pCAMBIA1302 with a 3×Flag-tag was used as expression vector, and at least two generations of resistance screening were carried out. All plants were grown in a growing chamber at 21–22°C with cool-white fluorescent light (80–100 μmol $m^{-2}s^{-1}$) in a long day photoperiod (16 h light/8 h dark). Arabidopsis

Seedlings were cultivated for 7 days in half-strength Murashige and Skoog (1/2 MS medium) supplemented with 0.6% (w/v) sucrose and 0.7% (w/v) agar, and then transferred to 1/2 MS medium with 0, 75, 150 μM $CdCl_2$ for another 7 days in growth chamber. The measurement of seedling root length and fresh weight and statistics of survive rate were performed after 7 days treatment in 1/2 MS medium. At the same time, one-week old Arabidopsis plants were cultivated in garden soil (Basic substrate No. 1, Pindstrup Mosebrug A/S, Denmark) without additional fertilizer for Cd stress treatment. Young plants were grown for three weeks in garden soil, and then used for Cd treatment by watering with and without 150 μM $CdCl_2$ solution, respectively.

Full length of *TaSBP-A* CSD was cloned into wheat expression vector, pWMB110, with a HA tag under the control of maize *UBI* promoter. The new vector was transformed into *Agrobacterium tumefaciens* strain C58C1 by triparental mating, and then further introduced into W48 immature embryos to generate transgenic plants according to the methods described by previous report (Wang et al., 2017a). The mature seeds from three independent stable transgenic lines at T3 generation were geminated in filter paper soaked with distilled water. After 48 h, uniformly germinated seeds were selected to grow in the half strength Hoagland's nutrient solution. Cd stress treatment was applied to W48 (non-transgenic control) and *TaSBP-A* overexpressed wheat seedlings at three-leaf stage with 0 and 50 μM $CdCl_2$ for two weeks. The measurement of the fresh weight and root length were performed after 2 weeks treatment. The seedling leaves and roots were respectively collected for the measurement of Cd content.

Measurements of chlorophyll, malondialdehyde and H_2O_2 content, SOD activity and chlorophyll fluorescence

Wild-type and transgenic Arabidopsis plants were treated with 150 μM Cd for 4 weeks. The measurement of chlorophyll and malondialdehyde (MDA) content and the detection of superoxide dismutase (SOD) activity were carried out according to previous report (Li et al., 2017). H_2O_2 content was measured using kit (KGT018, KeyGen Biotech, China) based on the manufacturer's instructions. Chlorophyll fluorescence was detected by using IMAGING-PAM chlorophyll fluorometer (Walz, Effeltrich, Germany) as previous report (Schreiber et al., 2007). The wild-type and transgenic plants were treated by 20 photons $m^{-2}•s^{-1}$ (actinic light) after dark-adaptation. And then maximal PSII quantum yield (F_v/F_m) was measured. The equation was used to calculate F_v/F_m : $F_v/F_m = (F_m–F_0)/F_m$. The effective PSII quantum yield (ΦPSII) was determined by using the formula: $ΦPSII = (F_m'-F)/F_m'$. The inhibition of PSII quantum yield (Inh) was detected by using the equation: Inh = (ΦPSII control–ΦPSII sample)/ΦPSII control.

Measurement of total Cd content in yeast cells and plant extracts

Cd-treated and untreated yeast cells and plant leaves were washed with Cd^{2+} free medium or ddH_2O, and dried for 3 d at 55°C, and then put into digestion tank. Pre-digesting was conducted by adding 5 mL 65% HNO_3 (Suprapur; Merck) and 2 mL H_2O_2 (Suprapur; Merck) to the digestion tank for 40 min at room temperature. The samples were digested by microwave digestion instrument (MARS, CEM Corporation, USA) for 2 h. Cd content (ng/g DW) was calculated using inductively couple mass spectrometry (ICP-MS, ELAN DRC-e, PerkinElmer) according to previous report (Maher et al., 2001).

Measurement of Cd^{2+} fluxes and Cd microscopic imaging

Cd^{2+} fluxes from one-week-old Arabidopsis seedlings cultivated on 1/2 MS were detected. Net fluxes of Cd^{2+} in root hair were measured by the noninvasive micro-test technique (NMT; BIO-001A, Younger United States Science and Technology Corp, Beijing, China) combined with IFLUXES/IMFLUXES 2.0 software (NMT100 Series, Younger USA, Amherst, MA, USA) (Ma et al., 2015). The microelectrodes were calibrated in 0.1 and 0.01 mM Cd^{2+} before the measurements of Cd^{2+} flux. The electrodes with Nernstian slopes were > 29 ± 3 mv/decade. Arabidopsis seedlings were transferred into a measuring chamber containing 10 mL of measuring solution (0.1 mM KCl, 0.03 mM $CdCl_2$, and 0.3 mM MES, pH 5.8.) and equilibrated for 10 min before measurement.

Visualization of free Cd^{2+} in Arabidopsis roots was conducted in one-week-old seedlings. The Cd probe Leadmium™ Green AM dye (Molecular Probes, Invitrogen, Calsbad, CA, USA) was utilized to detect the distribution of Cd in plant roots pre-treated with 150 μM Cd^{2+} for 0, 6 and 12 h. Cd fluorescence was excited at 488 nm and visualized using Zeiss LSM 780 (Carl Zeiss, Germany).

Overexpression of TaSBP-A/ΔTaSBP in *E. coli* and purification of the recombinant proteins

The mutant (ΔTaSBP-A) with displaced Cys with Gly in the putative metal binding regions was constructed. cDNA in the entry clone was cloned into the destination vectors pEGX-4T-1, used to produce GST-TaSBP-A/ΔTaSBP protein carrying additional 250 amino acids at the N terminus compared to the recombinant proteins. The recombinant plasmids were transformed into *E. coli* strain BL21. The cell cultures were fostered at 37°C for 3-4 h until the OD = 0.6-0.8, and then 1 mM IPTG was added for induction 16 h at 16°C. The recombinant proteins were isolated by batch purification with glutathione sepharose 4B according to the manufacturer's instructions (Amersham). Protein concentrations were determined by spectrophotometer (NanoDrop 2000, Thermoscientific) at 280 nm.

In vitro Cd^{2+} binding shift and binding ratio measurement

Two constructs wild type with the normal CXXC motif (TaSBP-A) and mutant with the GXXG motif (ΔTaSBP-A) were prepared.

The recombinant protein (100 μM) of TaSBP-A/ΔTaSBP was incubated with 500 μM $CdCl_2$ and 500 μM $CdCl_2$ together with 500 μM EDTA at 4°C overnight. The shift was tested by using 10% SDS-PAGE. The recombinant plasmid of pEGX-*TaSBP-A/ΔTaSBP* was transformed into *E. coli* BL21 (DE3) and induced at 16°C for 10 h with 1 mM IPTG. Then, 100 μM $CdCl_2$ was added to the liquid medium for 10 h culture. The cells were collected and mildly lysed using BugBuster Master Mix (Novagen, 71456-4). The lysis was centrifuged at 16000 g and 4°C for 15 min. The purified proteins were divided into equal two parts: one used for measuring Cd content by ICP-MS, and the other for measuring the protein concentration by DC protein determination kit (Bio-Rad). The stoichiometry of protein binding to Cd was conducted according to Cd and protein concentration (Luo et al., 2019).

Thermodynamic parameters determined by isothermal titration calorimetry and secondary structure characterization by circular dichroism

Cd-TaSBP-A/ΔTaSBP thermodynamic parameters were detected by calorimetric experiments of the recombinant TaSBP-A/ΔTaSBP proteins. Calorimetric titrations were conducted at 25°C with stirring at 1000 rpm with a filter time constant of 2 s by using a microcalorimeter (Microcal ITC 200 System, GE Healthcare). Negative controls were performed by the injections into the buffer, resulting only in signals from heat of salt dilution.

Secondary structure characterization (modifications) of the recombinant TaSBP-A protein after incubation with Cd^{2+} was performed by circular dichroism (CD). The recombinant protein of TaSBP-A/ΔTaSBP (1 nmol) was incubated with gradient concentration of Cd^{2+} (0, 2, 3, 4 nmol) in 250 μL incubation buffer. Spectra acquisition at 25°C used a spectropolarimeter (J-815, Jasco) at the far UV (200–260 nm). The following parameters were set: 1 nm step, 2 nm band width, and scan speed 200 nm/min with the optical path length 1 mm. The assessment of protein second structure was performed by K2D method based on the linear regression method (Yang et al., 1986).

Genetic transformation of TaSBP-A and ΔTaSBP-A in wheat protoplasts and viability comparison under Cd treatment

The wheat protoplasts were cultivated overnight after transformation of plasmids including 16318hGFP, reconstructive *TaSBP-A* and *ΔTaSBP-A*, respectively. Then, the viable protoplasts were treated with 50 μM $CdCl_2$ for 0, 2, 4, 6, 8, 10, and 12 h. To determine cell viability, the GFP fluorescence and chloroplast autofluorescence were observed by confocal laser scanning microscope (Leica TCS SP5, Germany). The transgenic protoplasts were cultivated in 0 μM $CdCl_2$ as the control (CK). The relative rate of protoplasts viability (treatment group/CK) was counted from 0 to 12 h.

Results

Phylogenetics and structural characterization of TaSBPs

Three protein sequences (TraesCS3A01G422100.1, TraesCS3B01G457600.1 and TraesCS3D01G417500.1) in Chinese Spring Protein database (http://plants.ensembl.org/index.html) were homologous to Arabidopsis SBPs (AtSBP1/2/3); in turn, they respectively located on chromosomes 3A, 3B and 3D. Specifically, TraesCS3A01G422100.1 showed 98.59% and 97.37% identities to TraesCS3B01G457600.1 and TraesCS3D01G417500.1, respectively (Figure S1). This demonstrates that hexaploid wheat had only three SBP copies, and they are named TaSBP-A, TaSBP-B and TaSBP-D. A phylogenetic tree constructed by 11 SBPs from different animal and plant species showed that TaSBP-A/B/D had a close phylogenetic relationship with the SBP56 family (Figure 1A).

Structural characterization showed that TaSBPs belonged to the SBP56 family and contained a putative heavy metal binding motif as well as a selenium-binding site CXXC (Figure 1B). They also showed a partial similarity with other typical metal binding proteins in the metal binding region CXXC (Figure 1C). A three-dimensional model analysis of TaSBP-A was performed by using SWISS-MODEL (https://swissmodel.expasy.org/) to identify the potential Cys residues involved in Cd binding. As the closest homologue, the structure of the hypothetical selenium-binding protein from *Sulfolobus tokodaii* (SMTL ID: 2ece.1) was used to generate a three-dimensional model with the program Modeler (Global Model Quality Estimation of 0.7; 43.91% sequence identity). As shown in Figure 1D, nine potential Cys residues were located on the surface of the TaSBP-A protein, among which four Cys residues, Cys^{100}, Cys^{102}, Cys^{161}, and Cys^{488}, showed high conservation. Cys^{23} and Cys^{24} were conserved in all the photosynthetic organisms, which were identified as the selenium-binding sites in Arabidopsis (Schild et al., 2014). The Cys^{100} and Cys^{102} on the random coil belonged to a CXXC motif related to metal binding (Lin and Culotta, 1995; Yuan et al., 1995; Culotta et al., 1997).

Expression and subcellular localization of TaSBP-A

RNA-seq analysis of the three *TaSBPs* in different organs of wheat showed that all *TaSBPs* expressed in root, stem and leaf. Of these, *TaSBP-A* had the highest expression level in three organs, particularly in the plant root (Figure 1E). Further RT-qPCR analysis displayed a similar expression pattern in different plant organs (Figure 1F). According to the above results, we chose *TaSBP-A* for further functional survey. *TaSBP-A* consisted of 1485 bp encoding 495 amino acid residues, and the deduced molecular mass was 54.1 kDa without considering protein modification.

To determine the subcellular location of the TaSBP-A, a *TaSBP-A-GFP* fusion vector (pTaSBP-A-GFP) driven by two CaMV35S promoter was constructed and transformed into wheat protoplasts. In cells only expressing GFP, the entire cytoplasm and nucleus were

10.3389/fpls.2023.1103241

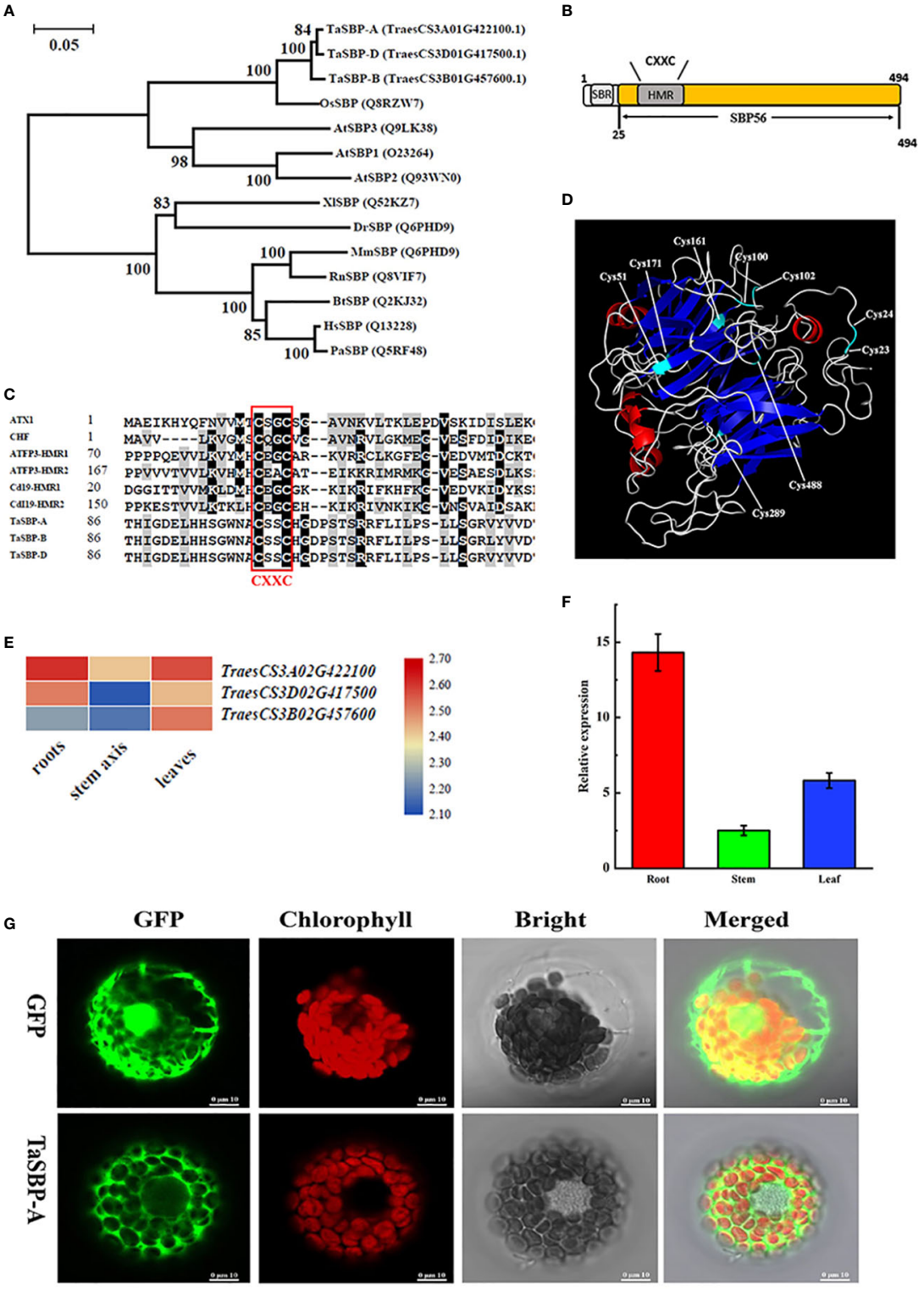

FIGURE 1
Phylogenetics and structural characterization of wheat TaSBPs. **(A)** Phylogenetic relationships between TaSBP-A/B/D protein and other SBPs of various species. **(B)** Simplified illustration of TaSBP protein structure. One putative metal binding region (HMR) and one Selenium-binding region (SBR) are shown. **(C)** Protein sequences containing the CXXC-type metal binding domain were acquired from GenBank. Accession numbers include ATX1 (P38636), CHF (AAC33510), ATFP3 (AAD09507) and Cd19 (AAM64219.1). The core sequence of the metal binding region is CXXC (here C represents cysteine and X represents any amino acid). **(D)** 3-D structure of TaSBP-A based on the structure of *S. tokodaii* (SMTL ID: 2ece.1). **(E)** The heat map of *TaSBP's* expression in the root, stem and leaf of wheat seedings. **(F)** The expression of *TaSBP-A* in different organs of *Chinese Spring* at the three-leaf stage. **(G)** Subcellular distribution of the 35S-TaSBP-GFP fusion proteins in wheat protoplasts as shown by confocal laser scanning microscope. The red represents the chloroplast fluorescence and the green indicates the GFP fluorescence.

diffusely labeled by a laser scanning microscopy. In contrast, the GFP fluorescence of TaSBP-A-GFP was only visible at cytoplasm, which clearly indicates that the TaSBP-A was localized in the cytoplasm (Figure 1G).

Cd stress response of TaSBP-A in wheat and overexpressed yeast cells

The *TaSBP-A* expression in response to Cd stress in the seedling roots of Chinese Spring was detected by both RT-qPCR (Figure 2A) and Western blot (Figure 2B). The results showed that both transcription and translation expression levels of TaSBP-A were significantly induced by time increasing under Cd stress (Figures 2A, B). In particular, both transcription and translation of TaSBP-A arrived at the highest level at 72h compared with control (24h), suggesting that TaSBP-A can be induced and accumulated in roots by Cd stress and may have potential roles in Cd stress response.

Because yeast has no SBP homolog, we overexpressed the *TaSBP-A* in yeast to detect the Cd tolerance of yeast cells. As shown in Figure 2C, EV and *TaSBP-A* yeast cells had a practically equal growth rates under normal condition; however, the *TaSBP-A* cells showed a higher growth rate than did the *EV* cells under 30 μM Cd^{2+} treatment (Figure 2C). Subsequently, we respectively cultured *EV* and *TaSBP-A* cells in a liquid medium containing 25 μM $CdCl_2$; here, the Cd content in yeast was detected by ICP-MS. Interestingly, the *TaSBP-A* overexpression in yeast could accumulate more Cd than EV significantly, as shown to be by 10.8% (Figure 2D). These results indicated that *TaSBP-A* can enhance the Cd tolerance of yeast cells by binding toxic free Cd ions.

The constitutive heterologous expression of TaSBP-A alleviated the oxidative stress and photosynthesis impairment triggered by Cd treatment in Arabidopsis

To reveal *TaSBP-A* function in the response to Cd stress, we further overexpressed it in Arabidopsis. Three stable overexpressed transgenic lines (S2-9, S3-12 and S4-7) were generated using genome PCR and western blot detection (Figures S2A-C). The overexpression protein level of TaSBP-A is S4-7 < S2-9 <S3-12 (Figure S2C). The seedlings of the *TaSBP-A* transgenic lines and wild type (WT) were cultivated on 1/2 MS containing 0, 75, and 150 μM $CdCl_2$ for 7 days.

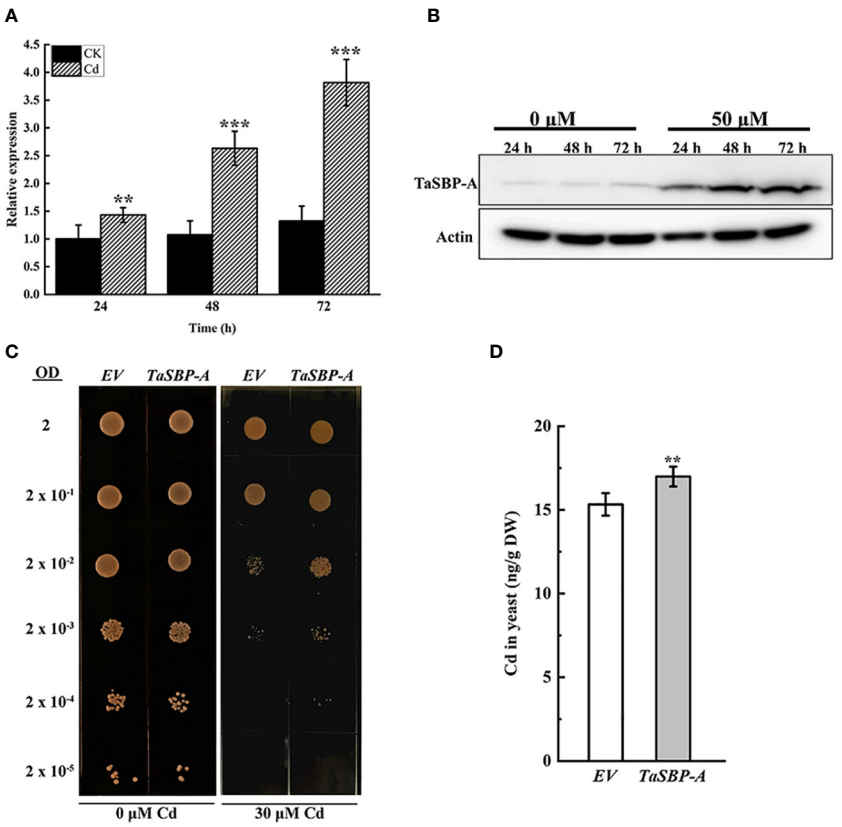

FIGURE 2
TaSBP-A responding to Cd-stress in Chinese Spring roots and its overexpression in *Saccharomyces cerevisiae* DEY1457. Wheat seedlings were treated with 50 μM $CdCl_2$ for 24, 48 and 72 h during the three-leaf stage. **(A)** Transcription expression by RT-qPCR. **(B)** Protein accumulation by Western blot. **(C)** Serial dilutions of the *S. cerevisiae* strains expressing the pYES2 empty vector (EV); a pYES2 harbouring one of the *TaSBP-A* spotted on medium supplemented with 0 (control) or 30 μM $CdCl_2$, as indicated at bottom of the panels. Each spot is comprised by 5 μl of a yeast culture diluted at the optical density at 600 nm (OD600 = 2.0 is the first spot). **(D)** Cd content of harvested cells measured by ICP-MS. A one-way ANOVA was used for the statistical analysis of the data. The asterisks represent the significant differences at different levels (**p<0.01; ***p<0.001).

The primary root growth was significantly inhibited and substantial chlorosis of cotyledons occurred in the WT plants (Figures S2D, E). However, *TaSBP-A* overexpressed seedlings maintained a higher fresh weight, root length and survival rate (Figures S2F-H), showing that all of lines have a palpable Cd tolerance. The Cd accumulation measurement revealed that the overexpression of *TaSBP-A* lines could accumulate a greater amount of Cd, specifically 1.13-1.23 times as high as WT (Figure S2I).

The Cd tolerance of *TaSBP-A* overexpressed lines grown in garden soil was further detected under 150 μM $CdCl_2$ treatment. Both transgenic lines and WT had no clear differences in the growth under normal conditions. However, under Cd stress, the WT plants showed chlorosis leaves and a severe reduction of growth (Figure 3A). In contrast, the *TaSBP-A* transgenic plants displayed a clear resistance to Cd stress even though some chlorosis leaves still occurred. Physiological and biochemical parameter analyses showed that SOD activity in *TaSBP-A* overexpressed lines was 2.36 times and the content of H_2O_2 and MDA were only 50% and 39% as compared to WT plants (Figures 3B-D). These results demonstrated that *TaSBP-A* transgenic plants could effectively promote SOD activity that would be able to alleviate the oxidative stress triggered by heavy-metal-induced H_2O_2. Cd accumulation in the roots of ICP-MS showed that the *TaSBP-A* transgenic lines accumulated more Cd, 1.23-1.64 times higher than WT (Figure 3E).

We also detected the impairment of photosynthesis as a result of Cd stress in transgenic plants. The results showed that the chlorophyll fluorescence parameters had no clear differences between WT and *TaSBP-A* overexpressed lines under normal conditions (Figure 3F). However, the maximum quantum yield of PSII photochemistry in the dark-adapted state (F_v/F_m) in the transgenic plant leaves under 150 μM Cd was higher than it was for WT (Figure 3G). In particular, the operating efficiency of PSII (ΦPSII) in three overexpression lines under Cd treatments was 22.25-28.80%, which was significantly higher than it was for WT (Figures 3F, H). Cd exposure significantly promoted the inhibition of PSII quantum yield (Inh) in the WT plant leaves, but it had no clear effects on transgenic plants (Figures 3F, I). Similarly, the chlorophyll content in the leaves had no significant differences between WT and the *TaSBP-A* transgenic lines after 4 weeks in normal growth conditions, while the *TaSBP-A* transgenic lines were significantly higher chlorophyll content under Cd stress: 1.95-2.95 times as high as WT (Figure 3J). These results indicate that the overexpression of *TaSBP-A* could significantly alleviated the photosynthesis impairment of plants under Cd stress treatment.

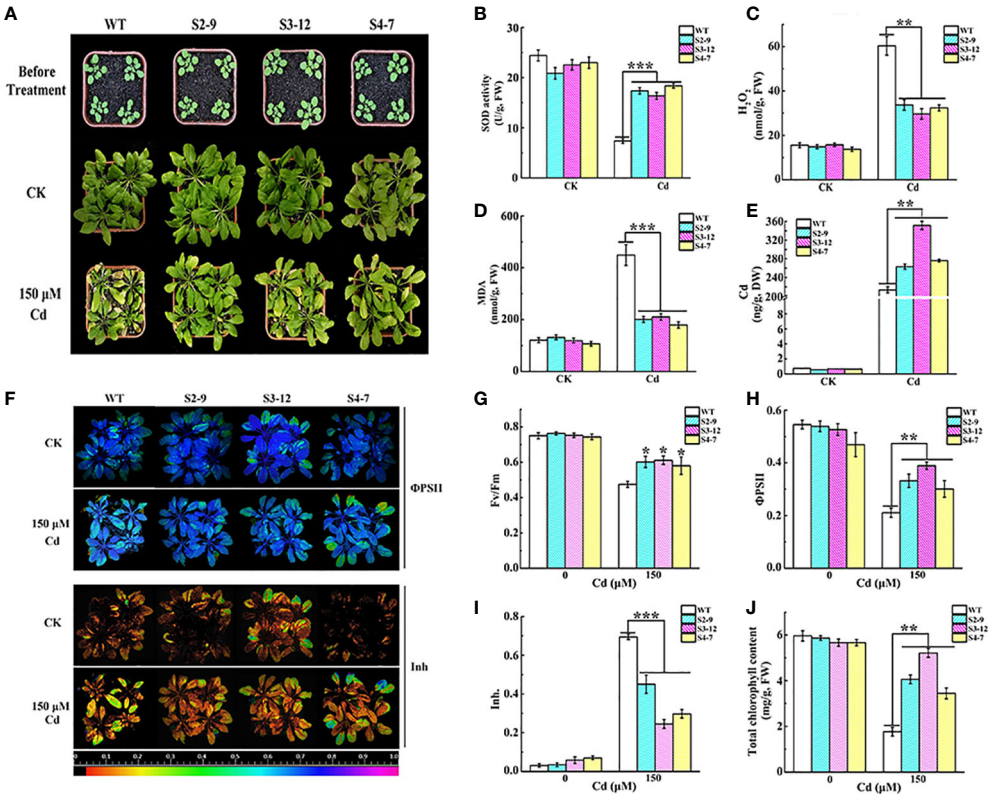

FIGURE 3
Overexpression of *TaSBP-A* alleviated the oxidative stress and photosynthesis impairment triggered by Cd treatment in Arabidopsis. **(A)** Phenotypic comparison of the wild type and transgenic Arabidopsis lines (S2-9, S3-12, and S4-7) under Cd stress. Three-week-old plants were watered with 150 μM $CdCl_2$ once a week for four weeks. Control group (CK) was normally irrigated with water. **(B–D)** Changes of SOD activity, H_2O_2 and the MDA content of transgenic Arabidopsis and the wild type (WT). **(E)** The Cd content changes in the roots of transgenic and wild type lines. **(F)** Chlorophyll fluorescence changes of the efficiency of PSII in the light (ΦPSII), and the inhibition of the PSII quantum yield (Inh.) of WT and overexpressed Arabidopsis lines. **(G–I)** Changes of chlorophyll fluorescence parameters F_v/F_m **(G)**, ΦPSII **(H)**, and Inh **(I)** extracted from fluorescence images. **(J)** Chlorophyll content changes of WT and the transgenic line under Cd stress. The data are indicated as mean± SD from three biological replicates. All data were statistically analyzed using a one-way ANOVA. The asterisks represent significant differences at different levels (*p< 0.05; **p< 0.01; ***p< 0.001).

Net fluxes and state of over-accumulated Cd^{2+} in transgenic Arabidopsis

As described above, *TaSBP-A* overexpression resulted in an increase of Cd accumulation in roots, thus we detected the net fluxes of Cd^{2+} in the root hairs of transgenic Arabidopsis under 30 μM Cd^{2+} using a noninvasive micro-test technique (Figure 4A). The results showed that the Cd^{2+} net fluxes in the root hairs of three transgenic lines S2-9, S3-12, and S4-7 were 2.49, 4.11 and 3.20 pmol $cm^{-2}{\cdot}s^{-1}$ respectively, which is 1.8-2.9 times higher than that of WT (Figure 4B). This confirmed that the overexpression of *TaSBP-A* could enhance the Cd^{2+} accumulation in roots of plant.

Leadmium™ Green AM dye, a Cd probe, was used to detect the state (free or binding) of the accumulated Cd, particularly with regard to the distribution of free Cd^{2+} in plant roots. As shown in Figure 4C, a very low level of green fluorescence was found in the roots of transgenic lines. This indicates that this dye has a high specificity to detect Cd^{2+} and that it does not react with divalent ions such as the Ca^{2+} present in the control roots. In contrast, the green fluorescence signals in WT plants appeared clearly above the hypocotyl after a 6 h pretreatment of 150 μM Cd^{2+}; they were more obviously enhanced after a 12 h pretreatment of 150 μM Cd in WT plants. However, the slight green fluorescence signals in the overexpression lines were only present below hypocotyl. These results indicated that overexpressed *TaSBP-A* played an important role in reducing free Cd^{2+} and that the over-accumulated Cd in the *TaSBP-A* overexpression lines was present largely in binding state.

Overexpressing TaSBP-A enhanced Cd tolerance by inhibiting the transfer of Cd from root to leaf in wheat seedlings

Three stable *TaSBP-A* overexpressed wheat lines, OVEREXPRESSION-1 (OE-1), OE-2 and OE-3, were obtained at

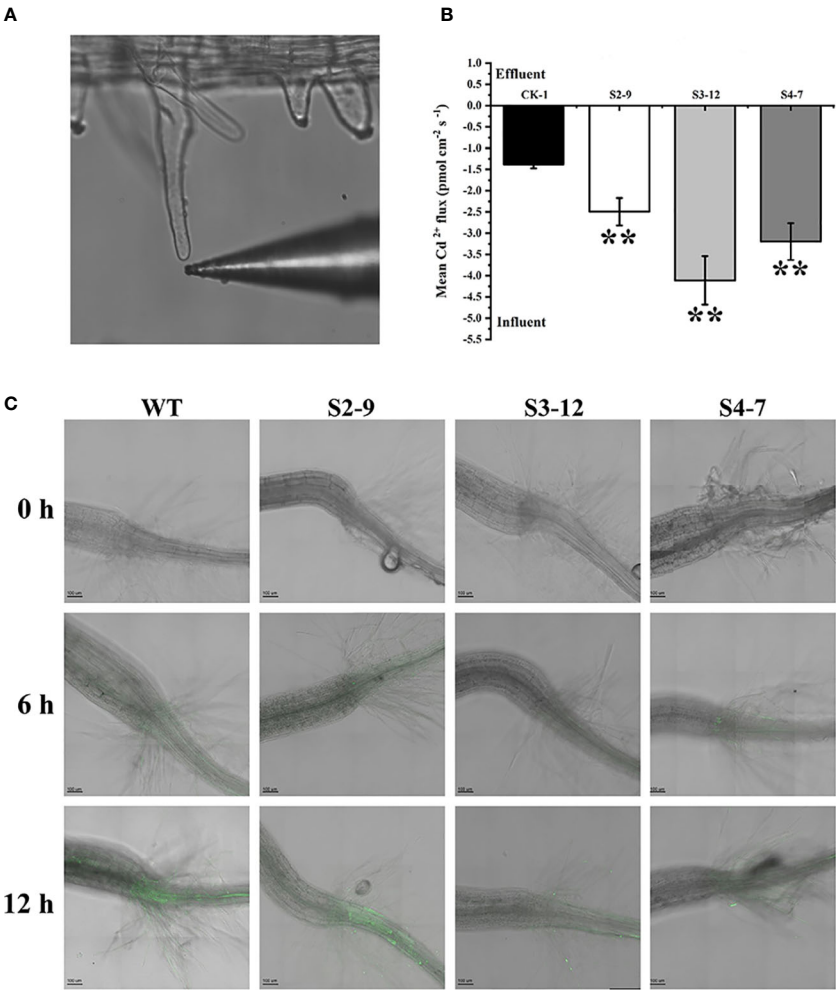

FIGURE 4
Cd^{2+} fluxes and free Cd^{2+} detection in *TaSBP-A* overexpressed Arabidopsis root hairs. **(A)** A representative root hair and the Cd^{2+}-selective microelectrode used. **(B)** The mean Cd^{2+} fluxes in the root hair was measured for 30 min after exposure to 30 μM Cd^{2+} by using a noninvasive micro-test technique. The data are indicated as mean± SD from the three biological replicates. All data were statistically analyzed using a one-way ANOVA. The asterisks represent significant differences at different levels (*p< 0.05; **p< 0.01; ***p< 0.001). **(C)** Micrographs of seedling roots from WT and overexpressed lines exposed to 150 μM Cd for different treatment times. Plant roots were pre-treated with 150 μM $CdCl_2$ for 0 h (control), 6 h and 12 h on a 1/2-MS plate and loaded with Leadamium™ Green AM dye for 60 min. All images were taken by a confocal laser scanning microscope (Leica TCS SP5, Germany). Green fluorescence indicates the binding of the dye to Cd.

T3 generation. The RT-qPCR and Western blot analysis showed both the transcription and translation expression levels of TaSBP-A were significantly higher in *TaSBP-A* overexpressed wheat seedlings than those in W48 seedlings (Figures 5B, C). The growth of W48 and *TaSBP-A* overexpressed wheat seedlings exposed to 0 and 50 μM $CdCl_2$ was compared after two weeks. Under normal condition, W48 and *TaSBP-A* overexpressed wheat seedlings showed a similar morphological characteristics (Figure 5A), and significant differences were not found in the fresh weight and root length between W48 and *TaSBP-A* overexpressed lines (Figure 5D, E). When subjected to 50 μM $CdCl_2$ treatment, a repressed growth was observed in both W48 and *TaSBP-A* overexpressed wheat seedlings, but W48 seedlings were more sensitive to Cd treatment (Figure 5A). The statistical analysis showed that both the fresh weight and root length of *TaSBP-A* overexpressed seedlings were higher than those in W48 seedlings (Figure 5D, E), indicating that *TaSBP-A* overexpressed wheat seedlings have a higher tolerance to Cd stress. In addition, the measurement of Cd content showed that a significantly higher amount of Cd was accumulated in the roots of *TaSBP-A* overexpressed wheat seedlings compared with W48 (Figure 5F). However, a lower amount of Cd was accumulated in the leaf of *TaSBP-A* overexpressed wheat seedlings (Figure 5G). These results indicated that overexpressed *TaSBP-A* could improve Cd tolerance of wheat seedlings by inhibiting the transfer of Cd from the root to leaf in wheat seedlings.

Determination of Cd-binding site in TaSBP-A

The above results indicated that TaSBP-A can enhance Cd tolerance of plants *via* reducing free Cd^{2+} and inhibiting the transfer of Cd from root to leaf. Thus, it is crucial to determine the Cd binding site in TaSBP-A in order to dissect the molecular

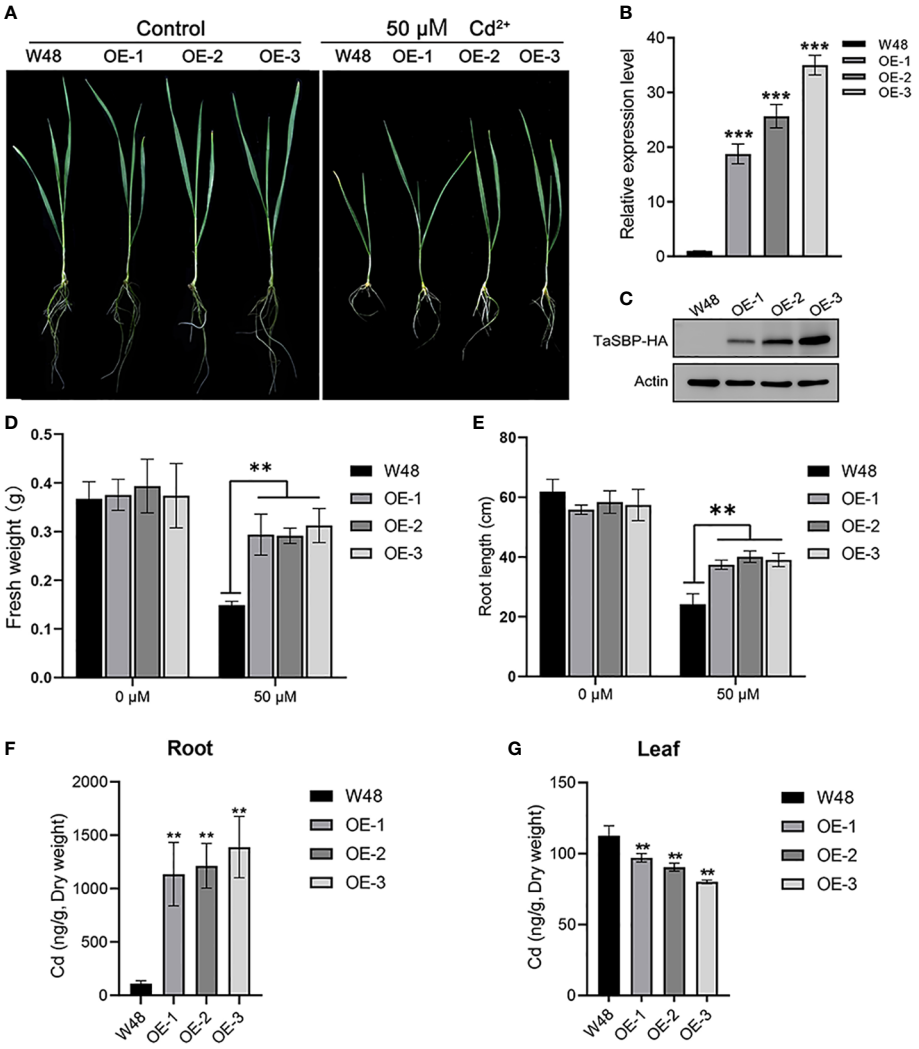

FIGURE 5
Overexpression of *TaSBP-A* enhanced wheat tolerance to Cd stress. **(A)** Seedlings of W48 and three *TaSBP-A* overexpressed lines (OE-1, OE-2 and OE-3) under 50 μM Cd^{2+} treatment for two weeks. **(B)** The expression levels of *TaSBP-A* relative to the internal control *UBI* gene in W48, OE-1, OE-2 and OE-3 determined by RT-qPCR. **(C)** The protein level of TaSBP-A-HA in leaf of W48 and *TaSBP-A* overexpressed wheat seedlings were validated using Western blot. **(D)** The fresh weight of plants under Cd stress. **(E)** The root length of plants under Cd stress. **(F)** The content of Cd in plant roots under 50 μM Cd^{2+} treatment for two weeks. **(G)** The content of Cd in plant leaves under 50 μM Cd^{2+} treatment for two weeks. The data are shown in mean values ± Sd. One-way ANOVA was used for statistical analysis of all data. The asterisks represent significant differences at different levels (**p< 0.01, ***p< 0.001).

mechanism of plant Cd-tolerance. The putative heavy metal binding motif CXXC (TaSBP-A) was mutated to GXXG (ΔTaSBP-A) and then the TaSBP-A and ΔTaSBP-A were respectively expressed in *E. coli* as a fusion protein with GST (Figure S3A). Subcellular localization indicated that the mutant of CXXC had no influence on the location of TaSBP-A (Figure S3B). Thus, we further conducted an *in vitro* Cd^{2+} binding assay according to the principle that ethylenediaminetetraacetic acid (EDTA) can chelate with Cd^{2+} to form Cd (II)-EDTA (Yang and Davis, 1999). As shown in Figure 6A, both recombinant TaSBP-A and ΔTaSBP-A had shifts in SDS-PAGE after incubation with 500 μM $CdCl_2$; in contrast, the shift disappeared with EDTA and the Cd coexistence in incubation buffer. However, after binding Cd^{2+}, it was hard to recognize the shift between TaSBP-A and ΔTaSBP-A. ICP-MS combined with protein quantification was further used to identify the stoichiometry of the interaction between Cd and protein, and the results showed that the stoichiometry of the TaSBP-A:ΔTaSBP-A binding to Cd was about 3: 2 (2.98: 1.59) (Figure 6B). This indicates that the ability of TaSBP-A decreased by

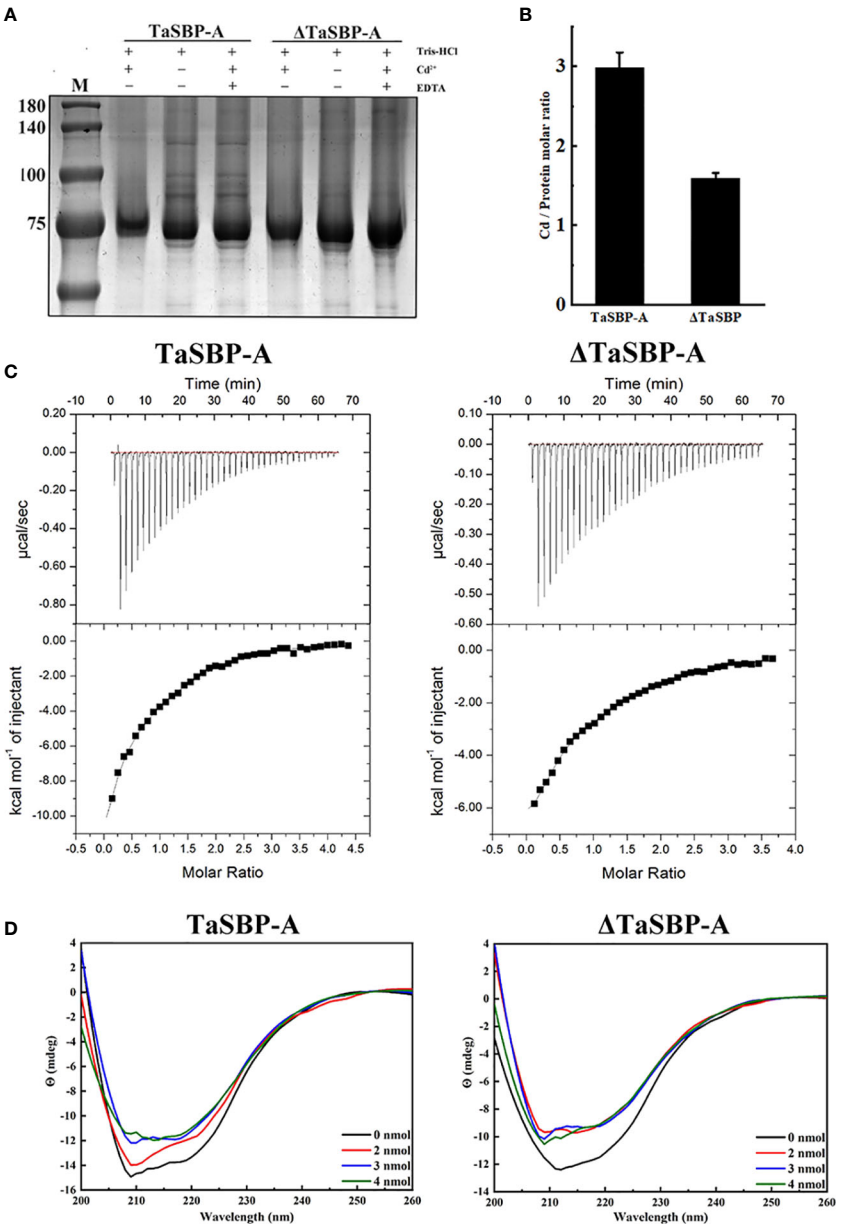

FIGURE 6
Determination of the Cd-binding site in TaSBP-A by *in vitro* Cd^{2+} binding assay. **(A)** Cd^{2+}-binding shift performed with 100 μM recombinant proteins and 0.5 mM Cd^{2+} *in vitro*. Tris-HCl was used as a reaction buffer and EDTA was used as a competitive inhibitor to protein. **(B)** The Cd/Protein Ratio determined by ICP-MS. **(C)** Isothermal titration calorimetry experiments of the recombinant TaSBP-A (left) and ΔTaSBP-A (right) binding to Cd. The top panel dispalys the titration of Cd^{2+} at 0.5 mM into TaSBP-A (ΔTaSBP-A) at 50 μM placed at the sample cell; the bottom panel indicates the ligand concentration dependence of the heat released upon binding after normalization. The data were fitted with the one-site binding model. The data are means ± SD from the three biological replicates. **(D)** CD spectra of the recombinant TaSBP-A (left) and ΔTaSBP-A (right) in the presence of a stepped Cd concentration (0-4 nmol Cd) at 25 °C. The protein content remained 1 nmol/250 μL during the whole experiment. The X and Y axes represent the wavelength (nm) and Y (mdeg), respectively.

47.3% after the CXXC motif mutation. This result further witnessed the interaction between TaSBP-A with Cd, where the CXXC motif served as the heavy metal binding site in the TaSBP-A.

Thermodynamic parameter analysis of the Cd^{2+} interactions with TaSBP-A and the impact of Cd^{2+}-binding on TaSBP-A's secondary structure

The interaction of Cd^{2+} with TaSBP-A and ΔTaSBP-A was detected by ITC. The ITC curves and thermodynamic parameters during the interaction of Cd^{2+} and TaSBP-A/ΔTaSBP-A are shown in Figure 6C and Table 1. For each Cd^{2+} injection, a release of heat was observed (Figure 6C, upper panel); this indicates that a clear binding event between Cd^{2+} and TaSBP-A/ΔTaSBP-A occurred. A one-site binding model was used to fit TaSBP-A/ΔTaSBP-A isotherms (Figure 6C, lower panel). This can determine an apparent binding affinity constant (K) in the low micromolar range (50 μM). Unexpectedly, the binding enthalpy value of the Cd^{2+} and TaSBP-A interaction was -17.92 kcal/mol, which was significantly higher than that of the Cd^{2+} and ΔTaSBP-A interaction (-13.30 kcal/mol) (Table 1). Therefore, we deduced that the two different strong negative enthalpy values (ΔH) for Cd^{2+} most likely correspond to a combination of a binding event with a specific covalent reaction between TaSBP-A/ΔTaSBP-A and Cd^{2+}. However, less heat was released in the interaction of ΔTaSBP-A with Cd^{2+}, which suggests that the Cd binding amount of TaSBP-A was palpably diminished after the mutation of the CXXC motif. The CXXC motif also witnessed entropy difference values (ΔS), a measurement for disorder and order in atomic and molecular assemblies (Landsberg, 1984). According to $\Delta S_{TaSBP\text{-}A} < \Delta S_{\Delta TaSBP\text{-}A}$, TaSBP-A was able to bind more Cd^{2+} than that of ΔTaSBP-A, leading to a dramatic decrease in ΔS. Furthermore, the calorimetric signals needed abnormally large amounts of time to recover to their baseline values after the CXXC motif mutation (Figure 6C) suggest that a covalent reaction combined with the binding of the ion was significant restrained due to the CXXC motif mutation in TaSBP-A. According to the K value, $K_{TaSBP\text{-}A}$ was 1.6 times as high as $K_{\Delta TaSBP\text{-}A}$ (Table 1), which is consistent with the results of the stoichiometry TaSBP-A/ΔTaSBP-A (Figure 6B). This indicates that the ability of TaSBP-A to bind to Cd was heavily suppressed after the loss of CXXC motif, which can reduce the affinity of other binding sites in TaSBP-A to Cd^{2+}.

CD analysis was used to further determine whether Cd-binding caused changes of the protein's secondary structure. The CD spectrum recorded the far-UV with TaSBP-A, ΔTaSBP-A, Cd-bound TaSBP-A and Cd-bound ΔTaSBP-A (Figure 6D) to estimate the second structure of proteins and Cd-proteins complexes. According to Table S1, the mutation of the CXXC motif had no effects on the β-sheet (about 45%) and turn (about 7.4%) content, but it resulted in an increase in random coil and a decrease in α-helix. With the presence of Cd^{2+}, the spectrum of TaSBP-A had more significant changes than did ΔTaSBP-A, indicating that the Cd-binding to TaSBP-A and the complex formation led to clear second structure alterations (Figure 6D). According to Table S1, the changes of TaSBP-A were obviously observed in the α-helix, β-sheet, turn and random coil content after binding to Cd^{2+}; in contrast, ΔTaSBP-A had only changes in turn content. These results showed that the significant changes of TaSBP-A's second structure occurred upon Cd^{2+} binding. Moreover, the CXXC motif was a crucial Cd^{2+}-binding site which could cause significant alterations of the protein's second structure as a result of interaction between TaSBP-A and Cd^{2+}.

In vivo validation of Cd-binding CXXC motif in wheat protoplasts

We transformed *TaSBP-A* and *ΔTaSBP-A* to wheat protoplasts for further Cd-binding CXXC motif and function verification of TaSBP (Figure S4). Empty vector 16318hGFP and recombinant plasmids containing *TaSBP-A* and *ΔTaSBP-A* were transformed into wheat leaves protoplasts, and then they were cultured with protoplasts culture medium with 50 μM Cd^{2+} (Figure S4A). The viable protoplasts (yellow light overlapped by chloroplast autofluorescence and GFP green fluorescence) that occurred after transformation were counted (Figure S4B). The transgenic efficiency of the empty vector was 27%, and it remained stable during the whole experiment under normal condition (0 μM Cd^{2+}). In turn, *TaSBP-A*/*ΔTaSBP-A* had a transform efficient of approximately 20%, serving as the basis to explore the relative rate of the protoplasts' viability (RRPV) under Cd treatment (Figure S4A). Compared to TaSBP-A (73%) and *ΔTaSBP-A* (56%), the number of viable protoplasts dramatically dropped after 12 h of Cd treatment in the empty vector, during which RRPV declined to 25% (Figure S4B). The dynamic RRPV was plotted from 0-12 h under cadmium treatment and it was also linearized (Figure 4B, Table S2). The results showed an order of $Slope_{EV} < Slope_{\Delta TaSBP\text{-}A} < Slope_{TaSBP\text{-}A}$ (-0.06306< -0.04225< -0.02226) (Table S2), which indicates that the death rate of protoplasts was EV> ΔTaSBP-A> TaSBP-A. Compared to *TaSBP-A*, the dynamic RRPV of *ΔTaSBP-A* transgenic cells during 0-4 h had no significant difference. However, after 4 h under Cd stress, the reduction of *ΔTaSBP-A* RRPV was more palpable than that of *TaSBP-A* (Figure S4). These results revealed that the CXXC motif played a key role in TaSBP tolerance to Cd stress, whose mutation can heavily inhibit the ability of TaSBP to interact with Cd^{2+}.

TABLE 1 Thermodynamic parameters calculated from micro-calorimetric experiments for the interaction between Cd^{2+} and TaSBP-A/ΔTaSBP-A at 25°C (298.15 K) in 10 mM HEPES, pH 7.4, 150 mM NaCl.

Proteins	K (M^{-1})	ΔH (kcal/mol)	ΔS (cal/mol/K)	ΔG (kcal/mol)
TaSBP-A	(33.2 ± 3.49) x 10^3	-17.92 ± 1.93	-39.4	-6.17 ± 1.93
ΔTaSBP-A	(20.7 ± 1.51) x 10^3	-13.30 ± 1.11	-24.9	-5.88 ± 1.12

Discussion

Abiotic stresses are the major adverse factors affecting crop yield. Thus, it is highly important for crop genetic improvement to discover potential stress-resistant genes and to explore the molecular mechanisms of plant adverse response. In particular, Cd severely affects the plant metabolic and physiological processes through elevating ROS (Ranieri et al., 2005) and through cell ultrastructural damages (Chen et al., 2018; Cheng et al., 2018). It can also enter chloroplasts and disturb chloroplast function by inhibiting the enzymatic activities in the chlorophyll biosynthesis and Calvin cycle, which leads to a decrease of chlorophyll content and photosynthesis (Ying et al., 2010). At the same time, excess Cd can cause overproduction of MDA content in wheat shoots and roots (Chen et al., 2010).

Plant SBPs can be induced by various stressors such as Cd, Se, Cu, Zn, and H_2O_2 (Dutilleul et al., 2008; Hugouvieux et al., 2009). We found that *TaSBP* genes expressed in different wheat organs; in particular, *TaSBP-A* had the highest expression level in the roots (Figures 1E, F). Similar to *AtSBP1* in Arabidopsis (Sarry et al., 2006; Dutilleul et al., 2008), *TaSBP-A*, as a highly hydrophilic cytosolic protein, was highly induced by Cd stress (Figure 2A, B). Its overexpression of yeast (Figures 2C, D), Arabidopsis (Figure S2, Figures 3, 4) and wheat (Figure 5) conferred Cd-tolerance through reducing free Cd^{2+} and inhibiting the transfer of Cd from root to leaf in plants. In addition, its overexpression contributed to photosynthesis impairment alleviation and ROS scavenging in Arabidopsis in our study. AtSBP1 protein could interact with AtGRXS14, which functions in redox state regulation in the chloroplasts (Valassakis et al., 2019). Taken together, the overexpression of TaSBP-A might enhance Cd tolerance in plant by two ways: one is regulation of redox state in chloroplasts by interaction with GRXS; the other is specific Cd-binding site present in TaSBP-A that directly interact with Cd to form a protein complex and, subsequently, to alleviate Cd toxicity.

The Cd toxicities are mainly brought up by free Cd^{2+}, which has a high ability to substitute other metals to serve as crucial active centers such as Cu in SOD and Mg in chlorophyll (Choppala et al., 2014). The loading of free Cd^{2+} into the root xylem can be mediated by heavy metal P_{1B}-ATPase, such as orthologues of HMA2 and HMA4 (Mendoza-Cózatl et al., 2011; Ismael et al., 2019). To date, the binding ability of SBPs to kinds of heavy metal such as Cd^{2+}, Zn^{2+} and Ni^{2+} has been reported by multiple researchers (Dutilleul et al., 2008; Schild et al., 2014). In this study, our results confirmed that *TaSBP-A* overexpression significantly reduced free Cd^{2+} content in plant roots (Figure 4C) as well as reduction of Cd content in wheat leaves (Figure 5G), which indicated that its overexpression might impede Cd long-distance translocation by chelation of free Cd^{2+} and lead to lower Cd content in overexpression wheat leaves than WT. Contaminated wheat and its products are some of the essential food contributors to dietary Cd intake by people (Abbas et al., 2017). Thus, it suggested that TaSBP may have potential to reduce Cd accumulation in grains.

In this study, we found the major existence of over-accumulated Cd occurred in the Cd-complexes (Figure 4), suggesting its strong binding ability to Cd. As a cytosolic protein, SBPs have a putative heavy metal binding motif CXXC that is highly conservative among different plant species (Figure S1). This motif contained two free accessible Cys residues on the random coils (Figure 1D), which may facilitate Cd-binding and protein complex formation. Many proteins containing the CXXC motif have been found to involve in metal ion metabolism and detoxification; this includes Cd19, MerP and ATX1 (Lin and Culotta, 1995; Powlowski and Sahlman, 1999; Suzuki et al., 2002). In this study, we provided sufficient evidence to confirm that the CXXC motif in TaSBP-A serves as a major Cd-binding site that can interact with Cd and form a metal complex to reduce the free Cd^{2+} content in root and decreased the amount of Cd^{2+} transferred from root to leaf in plants, and therefore alleviate the oxidative stress and photosynthesis impairment triggered by Cd stress.

We noticed that the mutation of CXXC to GXXG (ΔTaSBP-A) still had Cd-binding ability that caused some changes of the thermodynamic properties and the secondary structure of the recombinant proteins (Figures 6C, D; Table S1). This suggests that, in addition to the main CXXC binding site in TaSBP-A, other metal binding sites are still likely to be present. The side-chain carboxylate, sulfur and imidazole groups generally dominate metal coordination in proteins such as histidine, aspartic acid, glutamic acid and cysteine (Tainer et al., 1992). In particular, cysteine residues such as $Cys^{21}Cys^{22}$ for Se-binding in AtSBP1 were found to have binding ability (Schild et al., 2014). In addition, TaSBP-A had two more cysteine residues (Cys^{51} and Cys^{289}) than did AtSBPs. Thus, it can be excluded from the Cd-binding candidate sites with high probability due to its non-conservative characteristics (Figure S5). The β-sheet forms the framework for proteins and the loop between two β-sheets has high flexibility (Chothia et al., 1998). According to the predicted 3-D structure of TaSBP-A (Figure 1D), seven β-sheets provide the structural framework of TaSBP-A; in turn, this may cause more rigid structure for the residues located on β-sheet. Thus, the Cys^{161} and Cys^{171} located on β-sheet may be less flexible for Cd^{2+}-binding. The left cysteine residues (Cys^{23}, Cys^{24} and Cys^{488}) may serve as the candidate Cd-binding sites. In addition, three His-rich motifs (two HxD and one HxxH) are highly conserved in both TaSBPs and AtSBPs (Figure S5); as such, they may also serve as potential heavy metal binding sites (Flemetakis et al., 2002; She et al., 2003; Agalou et al., 2006). Further studies, however, are still needed to determine if this is the case.

In comparison with several micro-nutrients such as Zn, Mn and Ni, Cd translocation moves slowly from the root system to the shoot (Choppala et al., 2014). Almost 50% of the absorbed Cd is retained in the plant roots (Obata and Umebayashi, 1993). Harmful excess metal ions may enter cells *via* the cation transporters of the root tissues (Thomine et al., 2000). In order to deal with the damage inflicted by these absorbed metals, plants can produce metallochaperones to maintain appropriate levels of the metal concentration by binding and releasing (Suzuki et al., 2002). Subsequently, the bound metals may be transferred to metal trapping compounds such as phytochelatins, finally detoxifying them in vacuoles (Sanità Di Toppi and Gabbrielli, 1999; Cobbett and Goldsbrough, 2002; Wang et al., 2015). In this study, we found that the overexpression of *TaSBP-A* can cause higher absorption rates of Cd^{2+} as well as Cd^{2+}-locking under the hypocotyl of plant roots. Thus, TaSBP-A may serve as a cytoplasmic heavy metal transporter (metallochaperones) to help accelerate metal ion transport into the vacuole since the SBP56 family protein has a transport function that is involved in intra-Golgi protein transport (Porat et al., 2000).

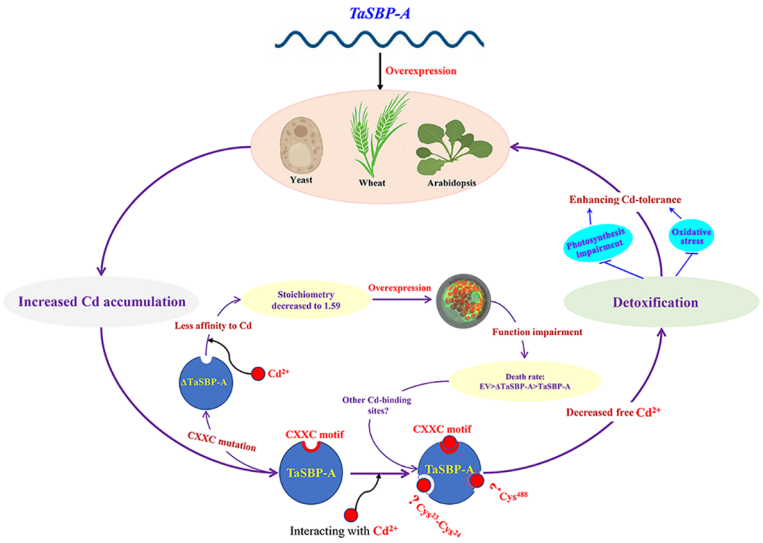

FIGURE 7
Schematic representation of TaSBP-A involved in Cd^{2+}-binding and detoxification in plants. The overexpression of *TaSBP-A* confers Cd-tolerance in yeast, Arabidopsis and wheat through the detoxification of free Cd^{2+}. The interaction between the CXXC motif and Cd enhances the sequestration of free Cd^{2+}, inhibits the Cd transfer from root to leaf and reduces the content of Cd^{2+} in plant leaf, ultimately conferring plant Cd-tolerance *via* alleviating the oxidative stress and photosynthesis impairment triggered by Cd stress.

In conclusion, as a cytoplasmic protein and typical SBP56 family member, TaSBP-A highly expressed in plant roots and it was highly induced by Cd stress. The overexpression of *TaSBP-A* conferred Cd-tolerance in yeast, Arabidopsis and wheat through the detoxification of free Cd^{2+}. The CXXC motif in TaSBP-A was confirmed as a major Cd-binding site *via* an *in vitro* Cd^{2+} binding assay in combination with a thermodynamics survey and a secondary structure analysis. The interaction between the CXXC motif and Cd as well as the metal protein complex formation enhanced detoxification of free Cd^{2+}, inhibited the Cd transfer from root to leaf and reduced the content of Cd^{2+} in plant leaf, ultimately conferring plant Cd-tolerance *via* alleviating the oxidative stress and photosynthesis impairment triggered by Cd stress (Figure 7).

Data availability statement

The datasets presented in this study can be found in online repositories. The names of the repository/repositories and accession number(s) can be found in the article/Supplementary Material.

Author contributions

FL, DZ and HS: Investigation, Writing-Original draft preparation. WD and JL: Investigation. YY: Conceptualization, Supervision, Writing- Reviewing and Editing. All authors contributed to the article and approved the submitted version.

Funding

This research was financially supported by grants from the National Key R & D Program of China (2016YFD0100502).

Acknowledgments

We thank Drs. Ke Wang and Xingguo Ye from Institute of Crop Sciences, Chinese Academy of Agricultural Sciences for the help of wheat genetic transformation. The English in this document has been checked by at least two professional editors, both native speakers of English. For a certificate, please see: https://submit.proofreadingmanuscripts.com/get-started.

Conflict of interest

The authors declare that the research was conducted in the absence of any commercial or financial relationships that could be construed as a potential conflict of interest.

Publisher's note

Supplementary material

The Supplementary Material for this article can be found online at: https://www.frontiersin.org/articles/10.3389/fpls.2023.1103241/full#supplementary-material

References

Abbas, T., Rizwan, M., Ali, S., Zia-ur-Rehman, M., Qayyum, M. F., Abbas, F., et al. (2017). Effect of biochar on cadmium bioavailability and uptake in wheat (Triticum aestivum l.) grown in a soil with aged contamination. *Ecotox Environ. Safe* 140, 37–47. doi: 10.1016/j.ecoenv.2017.02.028

Agalou, A., Spaink, H. P., and Roussis, A. (2006). Novel interaction of selenium-binding protein with glyceraldehyde-3-phosphate dehydrogenase and fructose-bisphosphate aldolase of arabidopsis thaliana. *Funct. Plant Biol.* 33, 847–856. doi: 10.1071/FP05312

Agami, R. A., and Mohamed, G. F. (2013). Exogenous treatment with indole-3-acetic acid and salicylic acid alleviates cadmium toxicity in wheat seedlings. *Ecotox Environ. Safe* 94, 164–171. doi: 10.1016/j.ecoenv.2013.04.013

Agarwal, P., Mitra, M., Banerjee, S., and Roy, S. (2020). MYB4 transcription factor, a member of R2R3-subfamily of MYB domain protein, regulates cadmium tolerance *via* enhanced protection against oxidative damage and increases expression of PCS1 and MT1C in arabidopsis. *Plant Sci.* 297, 110501. doi: 10.1016/j.plantsci.2020.110501

Arasimowicz-Jelonek, M., Floryszak-Wieczorek, J., and Gwóźdź, E. A. (2011). The message of nitric oxide in cadmium challenged plants. *Plant Sci.* 181, 612–620. doi: 10.1016/j.plantsci.2011.03.019

Bansal, M. F., Mukhopadhyay, T., Scott, J., Cook, R. G., Mukhopadhyay, R., and Medina, D. (1990). DNA Sequencing of a mouse liver protein that binds selenium: implications for selenium's mechanism of action in cancer prevention. *Carcinogenesis.* 11, 2071–2073. doi: 10.1093/carcin/11.11.2071

Bansal, M. P., Oborn, C. J., Danielson, K. G., and Medina, D. (1989). Evidence for two selenium-binding proteins distinct from glutathione peroxidase in mouse liver. *Carcinogenesis.* 10, 541–546. doi: 10.1093/carcin/10.3.541

Bhati, K. K., Alok, A., Kumar, A., Kaur, J., Tiwari, S., and Pandey, A. K. (2016). Silencing of ABCC13 transporter in wheat reveals its involvement in grain development, phytic acid accumulation and lateral root formation. *J. Exp. Bot.* 67, 4379–4389. doi: 10.1093/jxb/erw224

Cai, Z., Xian, P., Wang, H., Lin, R., Lian, T., Cheng, Y., et al. (2020). Transcription factor GmWRKY142 confers cadmium resistance by up-regulating the cadmium tolerance 1-like genes. *Front. Plant Sci.* 11. doi: 10.3389/fpls.2020.00724

Caparrós, P. G., Ozturk, M., Gul, A., Batool, T. S., Pirasteh-Anosheh, H., Unal, B. T., et al. (2022). Halophytes have potential as heavy metal phytoremediators: A comprehensive review. *Environ. Exp. Bot.* 193, 104666. doi: 10.1016/j.envexpbot.2021.104666

Cheng, Z. W., Chen, Z. Y., Yan, X., Bian, Y. W., Deng, X., and Yan, Y. M. (2018). Integrated physiological and proteomic analysis reveals underlying response and defense mechanisms of brachypodium distachyon seedling leaves under osmotic stress, cadmium and their combined stresses. *J. Proteomics* 170, 1–13. doi: 10.1016/j.jprot.2017.09.015

Cheng, Y., Yang, T., Xiang, W., Li, S., Fan, X., Sha, L., et al. (2021). Ammonium-nitrogen addition at the seedling stage does not reduce grain cadmium concentration in two common wheat (Triticum aestivum l.) cultivars. *Environ. pollut.* 286, 117575. doi: 10.1016/j.envpol.2021.117575

Chen, S., Yu, M., Li, H., Wang, Y., Lu, Z., Zhang, Y., et al. (2020). SaHsfA4c from sedum alfredii hance enhances cadmium tolerance by regulating ROS-scavenger activities and heat shock proteins expression. *Front. Plant Sci.* 11. doi: 10.3389/fpls.2020.00142

Chen, C. H., Zhou, Q. X., Cai, Z., and Wang, Y. Y. (2010). Effects of soil polycyclic musk and cadmium on pollutant uptake and biochemical responses of wheat (Triticum aestivum). *Arch. Environ. Contam Toxicol.* 59, 564–573. doi: 10.1007/s00244-010-9522-5

Chen, Z., Zhu, D., Wu, J., Cheng, Z., Yan, X., Deng, X., et al. (2018). Identification of differentially accumulated proteins involved in regulating independent and combined osmosis and cadmium stress response in brachypodium seedling roots. *Sci. Rep.* 8, 1–17. doi: 10.1038/s41598-018-25959-8

Chmielowska-Bąk, J., Gzyl, J., Rucińska-Sobkowiak, R., Arasimowicz-Jelonek, M., and Deckert, J. (2014). The new insights into cadmium sensing. *Front. Plant Sci.* 5. doi: 10.3389/fpls.2014.00245

Choppala, G., Bolan, N., and Park, J. H. (2013). Chromium contamination and its risk management in complex environmental settings. *Adv. Agron.* 120, 129–172. doi: 10.1016/B978-0-12-407686-0.00002-6

Choppala, G., Saifullah,, Bolan, N., Bibi, S., Iqbal, M., Rengel, Z., et al. (2014). Cellular mechanisms in higher plants governing tolerance to cadmium toxicity. *Crit. Rev. Plant Sci.* 33 (5), 374–391. doi: 10.1016/j.ecoenv.2015.06.003

Chothia, C., Gelfand, I., and Kister, A. (1998). Structural determinants in the sequences of immunoglobulin variable domain. *J. Mol. Biol.* 78, 457–479. doi: 10.1006/jmbi.1998.1653

Cobbett, C., and Goldsbrough, P. (2002). Phytochelatins and metallothioneins: Roles in heavy metal detoxification and homeostasis. *Annu. Rev. Plant Biol.* 53, 159–182. doi: 10.1146/annurev.arplant.53.100301.135154

Culotta, V. C., Klomp, L. W. J., Strain, J., Casareno, R. L. B., Krems, B., and Gitlin, J. D. (1997). The copper chaperone for superoxide dismutase. *J. Biol. Chem.* 272, 23469–23472. doi: 10.1074/jbc.272.38.23469

Dai, X., Feng, L., Ma, X., and Zhang, Y. (2012). Concentration level of heavy metals in wheat grains and the health risk assessment to local inhabitants from baiyin, gansu, China. *Adv. Mater.* 518, 951–956. doi: 10.4028/www.scientific.net/AMR.518-523.951

Dervisi, I., Valassakis, C., Agalou, A., Papandreou, N., Podia, V., Haralampidis, K., et al. (2020). Investigation of the interaction of DAD1-LIKE LIPASE 3 (DALL3) with selenium binding protein 1 (SBP1) in arabidopsis thaliana. *Plant Sci.* 291, 110357. doi: 10.1016/j.plantsci.2019.110357

Djemal, R., and Khoudi, H. (2022). The ethylene-responsive transcription factor of durum wheat, TdSHN1, confers cadmium, copper, and zinc tolerance to yeast and transgenic tobacco plants. *Protoplasma* 259, 19–31. doi: 10.1007/s00709-021-01635-z

Dutilleul, C., Jourdain, A., Bourguignon, J., and Hugouvieux, V. (2008). The arabidopsis putative selenium-binding protein family: expression study and characterization of SBP1 as a potential new player in cadmium detoxification processes. *Plant Physiol.* 147, 239–251. doi: 10.1104/pp.107.114033

Fatima, G., Raza, A. M., Hadi, N., Nigam, N., and Mahdi, A. A. (2019). Cadmium in human diseases: It's more than just a mere metal. *Indian J. Clin. Biochem.* 34, 371–378. doi: 10.1007/s12291-019-00839-8

Flemetakis, E., Agalou, A., Kavroulakis, N., Dimou, M., Martsikovskaya, A., Slater, A., et al. (2002). Lotus japonicus gene ljsbp is highly conserved among plants and animals and encodes a homologue to the mammalian selenium-binding proteins. *Mol. Plant Microbe* 15, 313–322. doi: 10.1094/MPMI.2002.15.4.313

Gratão, P. L., Monteiro, C. C., Tezotto, T., Carvalho, R. F., Alves, L. R., Peters, L. P., et al. (2015). Cadmium stress antioxidant responses and root-to-shoot communication in grafted tomato plants. *Biometals* 28, 803–816. doi: 10.1007/s10534-015-9867-3

Greger, M., and Löfstedt, M. (2004). Comparison of uptake and distribution of cadmium in different cultivars of bread and durum wheat. *Crop Sci.* 44, 501–507. doi: 10.2135/cropsci2004.5010

Grüter, R., Costerousse, B., Mayer, J., Mäder, P., Thonar, C., Frossard, E., et al. (2019). Long-term organic matter application reduces cadmium but not zinc concentrations in wheat. *Sci. Total Environ.* 669, 608–620. doi: 10.1016/j.scitotenv.2019.03.112

Haider, F. U., Liqun, C., Coulter, J. A., Cheema, S. A., Wu, J., Zhang, R., et al. (2021). Cadmium toxicity in plants: Impacts and remediation strategies. *Ecotoxicol Environ. Saf* 211, 111887. doi: 10.1016/j.ecoenv.2020.111887

Huang, Y., Wang, L., Wang, W., Li, T., He, Z., and Yang, X. (2019). Current status of agricultural soil pollution by heavy metals in China: A meta-analysis. *Sci. Total Environ.* 651, 3034–3042. doi: 10.1016/j.scitotenv.2018.10.185

Hugouvieux, V., Dutilleul, C., Jourdain, A., Reynaud, F., Lopez, V., and Bourguignon, J. (2009). Arabidopsis putative selenium-binding protein1 expression is tightly linked to cellular sulfur demand and can reduce sensitivity to stresses requiring glutathione for tolerance. *Plant Physiol.* 151, 768–781. doi: 10.1104/pp.109.144808

Ismael, M. A., Elyamine, A. M., Moussa, M. G., Cai, M., Zhao, X., and Hu, C. (2019). Cadmium in plants: uptake, toxicity, and its interactions with selenium fertilizers. *Metallomics.* 11, 255–277. doi: 10.1039/c8mt00247a

Jafarnejadi, A. R., Homaee, M., Sayyad, G., and Bybordi, M. (2011). Large Scale spatial variability of accumulated cadmium in the wheat farm grains. *Soil Sediment Contam* 20, 98–113. doi: 10.1080/15320383.2011.528472

Jianmin, Z., and Goldsbrough, P. B. (1994). Functional homologs of fungal metallothionein genes from arabidopsis. *Plant Cell.* 6, 875–884. doi: 10.1080/15320383.2011.528472

Jinadasa, N., Collins, D., Holford, P., Milham, P. J., and Conroy, J. P. (2016). Reactions to cadmium stress in a cadmium-tolerant variety of cabbage (Brassica oleracea l.): is cadmium tolerance necessarily desirable in food crops? *Environ. Sci. pollut. Res.* 23, 5296–5306. doi: 10.1007/s11356-015-5779-6

Kamran, A., Iqbal, M., and Spaner, D. (2014). Flowering time in wheat (Triticum aestivum l.): a key factor for global adaptability. *Euphytica* 197, 1–26. doi: 10.1007/s10681-014-1075-7

Khan, A., Khan, S., Khan, M. A., Qamar, Z., and Waqas, M. (2015a). The uptake and bioaccumulation of heavy metals by food plants, their effects on plants nutrients, and associated health risk: a review. *Sci. pollut. Res.* 22, 13772–13799. doi: 10.1007/s11356-015-4881-0

Khan, M. I. R., Nazir, F., Asgher, M., Per, T. S., and Khan, N. A. (2015b). Selenium and sulfur influence ethylene formation and alleviate cadmium-induced oxidative stress by improving proline and glutathione production in wheat. *J. Plant Physiol.* 173, 9–18. doi: 10.1016/j.jplph.2014.09.011

Kim, D. Y., Bovet, L., Maeshima, M., Martinoia, E., and Lee, Y. (2007). The ABC transporter AtPDR8 is a cadmium extrusion pump conferring heavy metal resistance. *Plant J.* 50, 207–218. doi: 10.1111/j.1365-313X.2007.03044.x

Korenkov, V., Hirschi, K., Crutchfield, J. D., and Wagner, G. J. (2007). Enhancing tonoplast Cd/H antiport activity increases cd, zn, and Mn tolerance, and impacts root/shoot cd partitioning in nicotiana tabacum l. *Planta* 226, 1379–1387. doi: 10.1007/s00425-007-0577-0

Landsberg, P. T. (1984). Can entropy and "order" increase together. *Phys. Lett. A* 102, 171–173. doi: 10.1080/15320383.2011.528472

Lang, I., and Wernitznig, S. (2011). Sequestration at the cell wall and plasma membrane facilitates zinc tolerance in the moss pohlia drummondii. *Environ. Exp. Bot.* 74, 186–193. doi: 10.1016/j.envexpbot.2011.05.018

Lei, G. J., Fujii-Kashino, M., Wu, D. Z., Hisano, H., Saisho, D., Deng, F., et al. (2020). Breeding for low cadmium barley by introgression of a sukkula-like transposable element. *Nat. Food.* 1, 489–499. doi: 10.1038/s43016-020-0130-x

Li, Y., Chen, Z., Xu, S., Zhang, L., Hou, W., and Yu, N. (2015). Effect of combined pollution of cd and B[a]P on photosynthesis and chlorophyll fluorescence characteristics of wheat. *Pol. J. Environ. Stud.* 24, 157–163. doi: 10.15244/pjoes/22274

Li, L., He, Z., Pandey, G. K., Tsuchiya, T., and Luan, S. (2002). Functional cloning and characterization of a plant efflux carrier for multidrug and heavy metal detoxification. *J. Biol. Chem.* 277, 5360–5368. doi: 10.1074/jbc.M108777200

Lin, S. J., and Culotta, V. C. (1995). The ATX1 gene of saccharomyces cerevisiae encodes a small metal homeostasis factor that protects cells against reactive oxygen toxicity. *Proc. Natl. Acad. Sci. U S A* 92, 3784–3788. doi: 10.1073/pnas.92.9.3784

Lin, J., Gao, X., Zhao, J., Zhang, J., Chen, S., and Lu, L. (2020). Plant cadmium resistance 2 (SaPCR2) facilitates cadmium efflux in the roots of hyperaccumulator sedum alfredii hance. *Front. Plant Sci.* 11. doi: 10.3389/fpls.2020.568887

Lin, T., Yang, W., Lu, W., Wang, Y., and Qi, X. (2017). Transcription factors PvERF15 and PvMTF-1 form a cadmium stress transcriptional pathway. *Plant Physiol.* 173, 1565–1573. doi: 10.1073/pnas.92.9.3784

Liu, N., Huang, X., Sun, L., Li, S., Chen, Y., Cao, X., et al. (2020). Screening stably low cadmium and moderately high micronutrients wheat cultivars under three different agricultural environments of China. *Chemosphere.* 241, 125065. doi: 10.1016/j.chemosphere.2019.125065

Li, Q., Zhang, X., Lv, Q., Zhu, D., Qiu, T., Xu, Y., et al. (2017). Physcomitrella patens dehydrins (PpDHNA and PpDHNC) confer salinity and drought tolerance to transgenic arabidopsis plants. *Front. Plant Sci.* 8. doi: 10.3389/fpls.2017.01316

López-Luna, J., Silva-Silva, M. J., Martinez-Vargas, S., Mijangos-Ricardez, O. F., González-Chávez, M. C., Solís-Domínguez, F. A., et al. (2015). Magnetite nanoparticle (NP) uptake by wheat plants and its effect on cadmium and chromium toxicological behavior. *Sci. Total Environ.* 565, 941–950. doi: 10.1016/j.scitotenv.2016.01.029

Luo, J. S., Yang, Y., Gu, T., Wu, Z., and Zhang, Z. (2019). The arabidopsis defensin gene AtPDF2.5 mediates cadmium tolerance and accumulation. *Plant Cell Environ.* 42, 2681–2695. doi: 10.1111/pce.13592

Ma, J., Cai, H., He, C., Zhang, W., and Wang, L. (2015). A hemicellulose-bound form of silicon inhibits cadmium ion uptake in rice (Oryza sativa) cells. *New Phytol.* 206, 1063–1074. doi: 10.1111/nph.13276

Maher, W., Forster, S., Krikowa, F., Snitch, P., Chapple, G., and Craig, P. (2001). Measurement of trace elements and phosphorus in marine animal and plant tissues by low-volume microwave digestion and ICP-MS. *Atom Spectrosc* 22, 360–371. doi: 10.46770/AS.2001.05.001

Ma, S., Nan, Z., Hu, Y., Chen, S., Yang, X., and Su, J. (2022). Phosphorus supply level is more important than wheat variety in safe utilization of cadmium-contaminated calcareous soil. *J. Hazard Mater.* 424, 127224. doi: 10.1016/j.jhazmat

Mendoza-Cózatl, D. G., Jobe, T. O., Hauser, F., and Schroeder, J. I. (2011). Long-distance transport, vacuolar sequestration, tolerance, and transcriptional responses induced by cadmium and arsenic. *Curr. Opin. Plant Biol.* 14, 554–562. doi: 10.1016/j.pbi.2011.07.004

Naeem, A., Zia-ur-Rehman, M., Akhtar, T., Zia, M. H., and Aslam, M. (2018). Silicon nutrition lowers cadmium content of wheat cultivars by regulating transpiration rate and activity of antioxidant enzymes. *Environ. pollut.* 242, 126–135. doi: 10.1016/j.envpol.2018.06.069

Najeeb, U., Jilani, G., Ali, S., Sarwar, M., Xu, L., and Zhou, W. (2011). Insights into cadmium induced physiological and ultra-structural disorders in juncus effusus l. and its remediation through exogenous citric acid. *J. Hazard Mater.* 186, 565–574. doi: 10.1016/j.jhazmat.2010.11.037

Obata, H., and Umebayashi, M. (1993). Production of SH compounds in higher plants of different tolerance to cd. *Plant Soil* 155, 533–536. doi: 10.1007/BF00025101

Ogawa, I., Nakanishi, H., Mori, S., and Nishizawa, N. K. (2009). Time course analysis of gene regulation under cadmium stress in rice. *Plant Soil* 325, 97–108. doi: 10.1093/pcp/pcv179

Pietrini, F., Zacchini, M., Iori, V., Pietrosanti, L., Ferretti, M., and Massacci, A. (2010). Spatial distribution of cadmium in leaves and its impact on photosynthesis: examples of different strategies in willow and poplar clones. *Plant Biol.* 12, 355–363. doi: 10.1111/j.1438-8677.2009.00258.x

Porat, A., Sagiv, Y., and Elazar, Z. (2000). A 56-kDa selenium-binding protein participates in intra-golgi protein transport. *J. Biol. Chem.* 275, 14457–14465. doi: 10.1074/jbc.275.19.14457

Powlowski, J., and Sahlman, L. (1999). Reactivity of the two essential cysteine residues of the periplasmic mercuric ion-binding protein, MerP. *J. Biol. Chem.* 274, 33320–33326. doi: 10.1074/jbc.274.47.33320

Qin, G., Niu, Z., Yu, J., Li, Z., Ma, J., and Xiang, P. (2021). Soil heavy metal pollution and food safety in China: Effects, sources and removing technology. *Chemosphere* 267, 129205. doi: 10.1016/j.chemosphere.2020.129205

Ranieri, A., Castagna, A., Scebba, F., Careri, M., Zagnoni, I., Predieri, G., et al. (2005). Oxidative stress and phytochelatin characterisation in bread wheat exposed to cadmium excess. *Plant Physiol. Biochem.* 43, 45–54. doi: 10.1016/j.plaphy.2004.12.004

Rizwan, M., Ali, S., Adrees, M., Ibrahim, M., Tsang, D. C., Zia-ur-Rehman, M., et al. (2017). A critical review on effects, tolerance mechanisms and management of cadmium in vegetables. *Chemosphere.* 182, 90–105. doi: 10.1016/j.chemosphere.2017.05.013

Rizwan, M., Meunier, J. D., Miche, H., and Keller, C. (2012). Effect of silicon on reducing cadmium toxicity in durum wheat (Triticum turgidum l. cv. Claudio w.) grown in a soil with aged contamination. *J. Hazard Mater.* 209, 326–334. doi: 10.1016/j.jhazmat.2012.01.033

Rousselot-Pailley, P., Sénèque, O., Lebrun, C., Crouzy, S., Boturyn, D., Dumy, P., et al. (2006). Model peptides based on the binding loop of the copper metallochaperone Atx1: selectivity of the consensus sequence MxCxxC for metal ions Hg (II), Cu (I), cd (II), Pb (II), and zn (II). *Inorg. Chem.* 45, 5510–5520. doi: 10.1021/ic060430b

Sanità Di Toppi, L., and Gabbrielli, R. (1999). Response to cadmium in higher plants. *Environ. Exp. Bot.* 41, 105–130. doi: 10.1016/S0098-8472(98)00058-6

Saraswat, S., and Rai, J. P. N. (2011). Complexation and detoxification of zn and cd in metal accumulating plants. *Rev. Environ. Sci. Bio* 10, 327–339. doi: 10.1007/s11157-011-9250-y

Sarry, J.-E., Kuhn, L., Ducruix, C., Lafaye, A., Junot, C., Hugouvieux, V., et al. (2006). The early responses ofArabidopsis thaliana cells to cadmium exposure explored by protein and metabolite profiling analyses. *Proteomics* 6, 2180–2198. doi: 10.1002/pmic.200500543

Sarwar, N., Saifullah,, Malhi, S. S., Zia, M. H., Naeem, A., Bibia, S., et al. (2010). Role of mineral nutrition in minimizing cadmium accumulation by plants. *J. Sci. Food Agric.* 90, 925–937. doi: 10.1002/jsfa.3916

Sawada, K., Hasegawa, M., Tokuda, L., Kameyama, J., Kodama, O., Kohchi, T., et al. (2004). Enhanced resistance to blast fungus and bacterial blight in transgenic rice constitutively expressing OsSBP, a rice homologue of mammalian selenium-binding proteins. *Bioscience Biotechnol. Biochem.* 68, 873–880. doi: 10.1271/bbb.68.873

Schild, F., Kieffer-Jaquinod, S., Palencia, A., Cobessi, D., Sarret, G., Zubieta, C., et al. (2014). Biochemical and biophysical characterization of the selenium-binding and reducing site in arabidopsis thaliana homologue to mammals selenium-binding protein 1. *J. Biol. Chem.* 289, 31765–31776. doi: 10.1074/jbc.M114.571208

Schreiber, U., Quayle, P., Schmidt, S., Escher, B. I., and Mueller, J. F. (2007). Methodology and evaluation of a highly sensitive algae toxicity test based on multiwell chlorophyll fluorescence imaging. *Biosensors Bioelectronics* 22, 2554–2563. doi: 10.1016/j.bios.2006.10.018

Shanying, H., Xiaoe, Y., Zhenli, H., and Baligar, V. C. (2017). Morphological and physiological responses of plants to cadmium toxicity: a review. *Pedosphere.* 27, 421–438. doi: 10.1016/S1002-0160(17)60339-4

She, Y.-M., Narindrasorasak, S., Yang, S., Spitale, N., Roberts, E. A., and Sarkar, B. (2003). Identification of metal-binding proteins in human hepatoma lines by immobilized metal affinity chromatography and mass spectrometry. *Mol. Cell Proteomics* 2, 1306–1318. doi: 10.1074/mcp.M300080-MCP200

Shim, D., Hwang, J.-U., Lee, J., Lee, S., Choi, Y., An, G., et al. (2009). Orthologs of the class A4 heat shock transcription factor HsfA4a confer cadmium tolerance in wheat and rice. *Plant Cell.* 21, 4031–4043. doi: 10.1105/tpc.109.066902

Suzuki, N., Yamaguchi, Y., Koizumi, N., and Sano, H. (2002). Functional characterization of a heavy metal binding protein CdI19 from arabidopsis. *Plant J.* 32, 165–173. doi: 10.1046/j.1365-313x.2002.01412.x

Tainer, J. A., Roberts, V. A., and Getzoff, E. D. (1992). Protein metal-binding sites. *Curr. Opin. Plant Biol.* 3, 378–387. doi: 10.1016/0958-1669(92)90166-G

Thomine, S., Wang, R., Ward, J. M., Crawford, N. M., and Schroeder, J. I. (2000). Cadmium and iron transport by members of a plant metal transporter family in arabidopsis with homology to nramp genes. *Proc. Natl. Acad. Sci. U S A* 97, 4991–4996. doi: 10.1073/pnas.97.9.4991

Uraguchi, S., Tanaka, N., Hofmann, C., Abiko, K., Ohkama-Ohtsu, N., Weber, M., et al. (2017). Phytochelatin synthase has contrasting effects on cadmium and arsenic accumulation in rice grains. *Plant Cell Physiol.* 58, 1730–1742. doi: 10.1093/pcp/pcx114

Valassakis, C., Dervisi, I., Agalou, A., Papandreou, N., Kapetsis, G., Podia, V., et al. (2019). Novel interactions of selenium binding protein family with the PICOT containing proteins AtGRXS14 and AtGRXS16 in arabidopsis thaliana. *Plant Sci.* 281, 102–112. doi: 10.1016/j.plantsci.2019.01.021

Verbruggen, N., Hermans, C., and Schat, H. (2009). Mechanisms to cope with arsenic or cadmium excess in plants. *Curr. Opin. Plant Biol.* 12, 364–372. doi: 10.1016/j.pbi.2009.05.001

Vitale, J., Adam, B., and Vitale, P. (2020). Economics of wheat breeding strategies: Focusing on Oklahoma hard red winter wheat. *Agronomy.* 10, 238. doi: 10.3390/agronomy10020238

Wang, P., Deng, X., Huang, Y., Fang, X., Zhang, J., Wan, H., et al. (2015). Comparison of subcellular distribution and chemical forms of cadmium among four soybean cultivars at young seedlings. *Environ. Sci. pollut. Res.* 22, 19584–19595. doi: 10.1007/s11356-015-5126-y

Wang, K., Liu, H., Du, L., and Ye, X. (2017a). Generation of marker-free transgenic hexaploid wheat *via* an agrobacterium-mediated co-transformation strategy in commercial Chinese wheat varieties. *Plant Biotechnol. J.* 15, 614–623. doi: 10.1111/pbi.12660

Wang, Z., Li, Q., Wu, W., Guo, J., and Yang, Y. (2017b). Cadmium stress tolerance in wheat seedlings induced by ascorbic acid was mediated by NO signaling pathways. *Ecotox Environ. Safe* 135, 75–81. doi: 10.1016/j.ecoenv.2016.09.013

Wei, J., Liao, S., Li, M., Zhu, B., Wang, H., Gu, L., et al. (2022). AetSRG1 contributes to the inhibition of wheat cd accumulation by stabilizing phenylalanine ammonia lyase. *J. Hazard Mater.* 428, 128226. doi: 10.1016/j.jhazmat.2022.128226

Xin, J., and Huang, B. (2014). Subcellular distribution and chemical forms of cadmium in two hot pepper cultivars differing in cadmium accumulation. *J. Agric. Food Chem.* 62, 508–515. doi: 10.1021/jf4044524

Xin, J., Huang, B., Dai, H., Liu, A., Zhou, W., and Liao, K. (2014). Characterization of cadmium uptake, translocation, and distribution in young seedlings of two hot pepper

cultivars that differ in fruit cadmium concentration. *Environ. Sci. pollut. Res.* 21, 7449–7456. doi: 10.1007/s11356-014-2691-4

Xu, Z., Liu, X., He, X., Xu, L., Huang, Y., Shao, H., et al. (2017). The soybean basic helix-loop-helix transcription factor ORG3-like enhances cadmium tolerance *via* increased iron and reduced cadmium uptake and transport from roots to shoots. *Front. Plant Sci.* 8. doi: 10.3389/fpls.2017.01098

Yang, J. K., and Davis, A. P. (1999). Competitive adsorption of Cu(II)-EDTA and Cd (II)-EDTA onto TiO2. *J. Colloid Interface Sci.* 216, 77–85. doi: 10.1006/jcis.1999.6278

Yang, W., and Diamond, A. M. (2013). Selenium-binding protein 1 as a tumor suppressor and a prognostic indicator of clinical outcome. *biomark. Res.* 1, 1–4. doi: 10.1186/2050-7771-1-15

Yang, G., Fu, S., Huang, J., Li, L., Long, Y., Wei, Q., et al. (2021). The tonoplast-localized transporter OsABCC9 is involved in cadmium tolerance and accumulation in rice. *Plant Sci.* 307, 110894. doi: 10.1016/j.plantsci.2021.110894

Yang, J. T., Wu, C. S. C., and Martinez, H. M. (1986). Calculation of protein conformation from circular dichroism. *Methods Enzymol.* 130, 208–269. doi: 10.1016/0076-6879(86)30013-2

Yao, X., Cai, Y., Yu, D., and Liang, G. (2018). bHLH104 confers tolerance to cadmium stress in arabidopsis thaliana. *J. Integr. Plant Biol.* 60, 691–702. doi: 10.1111/jipb

Ying, R. R., Qiu, R. L., Tang, Y. T., Hu, P. J., Qiu, H., Chen, H. R., et al. (2010). Cadmium tolerance of carbon assimilation enzymes and chloroplast in Zn/Cd hyperaccumulator picris divaricata. *J. Plant Physiol.* 167, 81–87. doi: 10.1016/j.jplph.2009.07.005

Yuan, D. S., Stearman, R., Dancis, A., Dunn, T., Beeler, T., and Klausner, R. D. (1995). The Menkes/Wilson disease gene homologue in yeast provides copper to a ceruloplasmin-like oxidase required for iron uptake. *Proc. Natl. Acad. Sci. U S A* 92, 2632–2636. doi: 10.1073/pnas.92.7.2632

Yu, Y., Zhu, D., Ma, C., Cao, H., Wang, Y., Xu, Y., et al. (2016). Transcriptome analysis reveals key differentially expressed genes involved in wheat grain development. *Crop J.* 4, 92–106. doi: 10.1016/j.cj.2016.01.006

Zaid, I., Zheng, X., and Li, X. (2018). Breeding low-cadmium wheat: progress and perspectives. *Agronomy.* 11, 249. doi: 10.3390/agronomy8110249

Zhang, L., Gao, C., Chen, C., Zhang, W., Huang, X.-Y., and Zhao, F.-J. (2020). Overexpression of rice OsHMA3 in wheat greatly decreases cadmium accumulation in wheat grains. *Environ. Sci. Technol.* 54, 10100–10108. doi: 10.1021/acs.est.0c02877

Zhang, M., Lv, D., Ge, P., Bian, Y., Chen, G., Zhu, G., et al. (2014). Phosphoproteome analysis reveals new drought response and defense mechanisms of seedling leaves in bread wheat (Triticum aestivum l.). *J. Proteomics* 109, 290–308. doi: 10.1016/j.jprot.2014.07.010

Zhou, M., and Li, Z. (2022). Recent advances in minimizing cadmium accumulation in wheat. *Toxics* 4, 187. doi: 10.3390/toxics10040187

Zou, R., Wu, J., Wang, R., and Yan, Y. (2020).). grain proteomic analysis reveals central stress responsive proteins caused by wheat-haynaldia villosa 6VS/6AL translocation. *J. Integr. Agric.* 19, 2628–2642. doi: 10.1016/S2095-3119(19)62846-7